भारत सरकार
GOVERNMENT OF INDIA
भाभा परमाणु अनुसंधान केन्द्र
BHABHA ATOMIC RESEARCH CENTRE

ESTIMATION AND ANALYSIS OF NEUTRON SKYSHINE AT
PARTICLE ACCELERATORS

by

G. Prabhakar Rao and P. K. Sarkar
Radiation Safety Systems Division

1998

29 - 35

GOVERNMENT OF INDIA
ATOMIC ENERGY COMMISSION

ESTIMATION AND ANALYSIS OF NEUTRON SKYSHINE AT PARTICLE ACCELERATORS

by

G. Prabhakar Rao and P.K. Sarkar
Radiation Safety Systems Division

BHABHA ATOMIC RESEARCH CENTRE
MUMBAI, INDIA

1998

BIBLIOGRAPHIC DESCRIPTION SHEET FOR TECHNICAL REPORT
(as per IS : 9400 - 1980)

01	Security classification :	Unclassified
02	Distribution :	External
03	Report status :	New
04	Series :	BARC External
05	Report type :	Technical Report
06	Report No. :	BARC/1998/E/003
07	Part No. or Volume No. :	
08	Contract No. :	
10	Title and subtitle :	Estimation and analysis of neutron skyshine at particle accelerators
11	Collation :	73 p., 5 figs.
13	Project No. :	
20	Personal author(s) :	G. Prabhakar Rao; P.K. Sarkar
21	Affiliation of author(s) :	Accelerator Radiation Protection Group at Variable Energy Cyclotron Centre, Calcutta, Radiation Safety Systems Division, Bhabha Atomic Research Centre, Mumbai
22	Corporate author(s) :	Bhabha Atomic Research Centre, Mumbai
23	Originating unit :	Radiation Safety Systems Division, BARC, Mumbai
24	Sponsor(s) Name :	Department of Atomic Energy
	Type :	Government

30	Date of submission :	January 1998
31	Publication/Issue date :	February 1998
40	Publisher/Distributor :	Head, Library and Information Division, Bhabha Atomic Research Centre, Mumbai
42	Form of distribution :	Hard Copy
50	Language of text :	English
51	Language of summary :	English
52	No. of references :	45 refs.
53	Gives data on :	

60   Abstract : This report deals with the neutron dosimetry at the accelerator environment with a special emphasis given to the neutron skyshine problem. Theoretical studies have been carried out for the estimation of neutron skyshine dose using experimentally measured neutron spectra as well as those obtained using theoretically simulated nuclear reaction model calculations. A detailed analysis has been performed with respect to several variables.

70   Keywords/Descriptors : NEUTRON DOSIMETRY; NEUTRON SPECTRA; NEUTRON TRANSPORT; MONTE CARLO METHOD; SHIELDING; SYNCHROTRON RADIATION; LINEAR ACCELERATORS; NEUTRON SPECTROSCOPY; P CODES; A CODES; CROSS SECTIONS; VALIDATION; DOSE RATES; SPECIFICATIONS; RECOMMENDATIONS; SUPERCONDUCTING CYCLOTRONS

71   Class No. :   INIS Subject Category : E1610

99   Supplementary elements :

ESTIMATION AND ANALYSIS OF NEUTRON SKYSHINE AT PARTICLE ACCELERATORS

G. Prabhakar Rao and P.K. Sarkar

gprao@veccal.ernet.in; pks@veccal.ernet.in

Accelerator Radiation Protection Group

Radiation Safety Systems Division

1/AF, Bidhan Nagar, Calcutta - 700 064.

Abstract: This report deals with the neutron dosimetry at the accelerator environment with a special emphasis given to the neutron skyshine problem. Theoretical studies have been carried out for the estimation of neutron skyshine dose using experimentally measured neutron spectra as well as those obtained using theoretically simulated nuclear reaction model calculations. A detailed analysis has been performed with respect to several variables.

Key Words: Neutron Skyshine, Accelerator Shielding.

Contents

List of Figures

1 Introduction

Neutron dose is the quantity used to describe the amount of energy imparted in terms of Joules/Kg in a body if exposed to a given fluence of neutrons and measurement of neutron dose is known as neutron dosimetry. The unit of neutron dose is Sv. This quantity depends on the number of neutrons falling on the body per unit area the energy of neutrons, and the quality factor for neutrons of that known energy. The quality factor is used to convert the physical quantity dose, to the corresponding biologically relevant quantity called effective dose. In practice, for the routine Health Physics purposes, calculation of effective dose in Sv is straight forward, if the neutron fluence and the corresponding energy is known. ICRP, (International Commission for Radiation Protection) recommended fluence to effective dose conversion factors over wide range of energies. The neutron dosimetry at different nuclear facilities like reactors, neutron generators, and accelerators differ only in the emitted neutron energy distribution. But, neutron interaction with different shield materials over several energy decades starting from thermal to several hundreds of MeV is not uniform, which makes the field of neutron dosimetry one of the complex subjects of nuclear technology. In this work, we deal with only neutron dosimetry at accelerator facilities. As has already been pointed out, neutron dosimetry depends not on the nuclear facility, but on the energy range of neutrons, and accelerators are the places where this variation of neutron energy is very large depending critically on the projectile-target combination. The neutron dosimetry inside any accelerator hall is not of much importance, except for the case of neutron radiation damage and activation products which are mostly short lived, and is due to two reasons.

- neutron field is mostly a prompt radiation field.

- accelerator will be well shielded and no occupancy is allowed during its operation.

Neutron dosimetry at far away distances is of great importance as it involves public and no radiation protection practices are carried out except for the control on the annual dose limits. The main purpose of radiation protection practices, is to protect all persons both operational and public from any uncontrolled excessive exposures. Neutron dosimetry at far away distances from an accelerator is mainly due to the air-scattered (multiple scatter) component which shines, instead of getting absorbed (the scattering cross-section is more in air than absorption because of low atomic number over a wide range of neutron energy) by the atmosphere during its course of nuclear interactions, and is rightly called **Neutron Skyshine**.

The long-range propagation of neutrons in the atmosphere and their scattering contributes significantly to the total external exposure of the nearby populations (Patterson and Thomas, 1973). The high radiation levels observed near particle accelerators built with insufficient roof shielding in the 1950's were attributed to these air scattered neutrons, otherwise known as skyshine neutrons (Lindenbaum 1957, 1961). It was found that the amount of skyshine depends on the source neutron characteristics (intensity, energy etc.) as well as on the thickness of the roof shields (Rindi and Thomas, 1975).

In recent years accelerators with increasing beam current and energy are being built in densely populated areas for medical, industrial and research purposes. Moreover, there is a growing concern recently in estimating and limiting population exposure resulting from nuclear installations. Systematic study of skyshine dose is thus important from the point of view of accelerator housing design. Several measurements have been carried out and many experimental skyshine doses have been reported. However, the large inherent inaccuracies in these measurements make any theoretical interpretation very difficult. In addition, in any measurement the topography and the presence of nearby buildings perturb the data. Also, it is not possible to carry out measurements for various roof thicknesses or for different source neutron spectra as produced in accelerators by different projectile-target combinations. It, therefore, becomes necessary to depend on computational techniques that are inexpensive and can furnish the required data with reasonable accuracy.

Detailed calculation using the Monte Carlo technique have been used since 1960 with more and more sophistication incorporated with advancing years (Trubey and Comolander, 1971; Nakamura and Kosako, 1981a). Though they simulated the problem very close to reality, these calculations are very expensive in terms of computer time and technique and therefore are inappropriate for a quick and detailed study of the variation of skyshine dose with respect to roof thickness, source spectrum etc. Such data are important for the engineers designing the accelerator building. The designers require a working knowledge as to which of these factors are important and to what extent for a safe design of the accelerator housing.

In this report we first review the earlier work in the field of nuetron skyshine calculations and then describe the developement a simple algorithm for the estimation of neutron skyshine. The source neutron spectrum is obtained using nuclear model calculations and subsequent neutron transport through the shield material using a one-dimensional neutron transport code. A detailed analysis has been to done with respect to the several parameters that affect it. We have carried out sensitivity studies to get an exact measure of the importance of neutron skyshine, which is known intuitively only.

2 A Brief Survey On The Estimation Of Neutron Skyshine Dose

2.1 First systematic study - Lindenbaum

Lindenbaum reported one of the first theoretical studies of the neutron skyshine phenomena at high-energy proton accelerators, and formulated an expression describing the propagation of low-energy neutrons (1-5 MeV) through the atmosphere. He has approximated the above problem using diffusion theory. The neutron flux produced by a point source in an infinite isotropic scattering medium, as derived by Case et al., (Case et al., 1953) is given by

$$\phi(r) = \frac{Q \exp(-\Sigma_t r)}{4\pi r^2}\epsilon(c,r) + \frac{QK(c)\exp(-K_0 r)}{4\pi Dr} \qquad (2.1)$$

- with Q = neutron source strength (n/s),

- Σ_t = total macroscopic cross-section (cm^{-1}),

- D = diffusion coefficient (cm),

- $1/K_0$ = diffusion length,

- $c = \Sigma_s / \Sigma_t$,

- r = distance from the source.

- $\epsilon(c,r)$ and $K(c)$ are empirical functions c.

The assumptions made in the Case formulation are:

- The above Eq. 2.1 is a solution for the diffusion of a mono-energetic neutron source, and they do not lose any kinetic energy in elastic collisions.

- The source is an isotropic point source.

- Neutrons diffuse in an infinite uniform absorbing medium (taken to be air by Lindenbaum).

- Scattering is isotropic in the center-of-the mass system.

The first term of Eq. 2.1 is almost identical with the equation describing the propagation of radiation from a point source with absorption but without scattering and becomes negligible for distances larger than 300m (about 3 mean free paths in air for neutrons in the energy range 1-5 MeV). The second term of Eq. 2.1 represents the component of the radiation field scattered to the point of measurement from all directions.

As described previously in the section 1, there is no precise definition of neutron skyshine and often refers to the radiation at a point away from a neutron source and includes direct component, majorly scattered component and also includes scattering from ground called **Ground Shine**. Given the situation of the complex neutron field near and at far away distances, Lindenbaum's expression is having limitations because of the above assumptions. Nevertheless, for practical health physics purposes (where a factor of 2 uncertainty is allowed) and when the shielding contains little or no hydrogen for example steel or lead as shielding material (which is majorly used in the electron synchrotron), Lindenbaum's expression can be used. When the accelerator is well shielded in the forward direction with earth or concrete, the radiation field is controlled by high-energy neutrons (>100 MeV), Lindenbaum's Eq. 2.1 can't predict neutron skyshine dose. Lindenbaum's expression was verified for low-energy neutrons using both experimental measurements (Kinney, 1962 ; Ladu et al., 1968) and using Monte Carlo studies of neutron transport for various mono-energetic neutron energies up to 20 MeV. Lindenbaum was the first to point out that at distances of several hundreds of meters from accelerators with no roof shielding, and at all distances from accelerators with roof shielding, high-energy neutrons (energy > 100 MeV) would control the radiation field. The importance of these high energy neutrons was also experimentally demonstrated.

2.2 Empirical formulation by Thomas.

Thomas has experimentally measured neutron skyshine at distances greater than 50 meters for a 50 MeV proton linear accelerator at the Rutherford Laboratory. He obtained an empirical expression (Thomas, 1968) that fits the experimental data, and is given by

$$\phi(r) = \frac{aQ}{4\pi r^2}(1 - \exp(-r/\mu)\,)\exp(-r/\lambda) \qquad (2.2)$$

where $r \geq 50$m, $a = 2.8$, $\mu = 56$m, and $\lambda = 267$m.

2.3 An actual skyshine experiment

In order to understand the radiation transport phenomena involved, one needs carefully controlled experiments which, in the competitive atmosphere of the front-line research accelerators, are difficult to carry out. Skyshine alone has been systematically studied probably for the first time by Hack (Hack, 1966) in possibly only one experiment at the 50 MeV proton linear accelerator of the Rutherford Laboratory. Neutrons were produced by stopping a 50 MeV proton beam in a thick aluminium target. Roof shielding was not provided but the target region was shielded with 0.9m (3ft) thick, 3.65m (12ft) high concrete walls. Measurements were made of the neutron dose equivalent, as a function of distance from the shield wall. The wall was then increased to 1.5m (5ft) thick and 3.65m (5ft) high and finally to 1.5m (5ft) thick and 5.8m (19ft) high. Figure 2.1 (borrowed from Rindi and Thomas, 1975) shows the neutron dose-equivalent rate as a function of distance from the shield. The upper curve shows that increasing the thickness of the shield from 0.9m (1 ft) to 1.5m (5 ft) had no significant effect on the radiation level, indicating that skyshine was the dominant source of neutrons. This was confirmed by measuring the dose-equivalent rate at a depth of 0.9m (3 ft) in the shield wall and outside the 1.5m (5 ft) shield wall. The dose rate at a depth of 0.9m(3ft) was less than 1% of the rate outside the shield wall. Figure 2.1 demonstrates the shadowing effect of the concrete wall, the maximum radiation level moving outwards as the wall height increases. Under such

conditions the observed neutron dose-equivalent is due to the neutrons scattered from the atmosphere back to the ground and can be truly described as **Skyshine**.

2.4 Neutron importance function

Neutron skyshine in terms of dose-equivalent can be obtained at an air-ground interface as a function of the distance from an assumed azimuthally symmetric point source. This can be calculated as a double integral, which is given as

$$D(\bar{r}) = \int S(E, \cos\theta) I(E, \cos\theta) dE \, d\theta \qquad (2.3)$$

where $S(E, \cos\theta)$, the number of source neutrons per unit solid angle at energy E, and polar angle θ (The source is by assumption independent of the azimuthal angle). $I(E, \cos\theta, \bar{r})$, the importance of neutron at energy, E and polar angle θ and average radial distance $\bar{r}$. Alsmiller et al., (Alsmiller et al., 1981) calculated the above quantity, $I(E, \cos\theta, \bar{r})$ and they named it as **Importance Function**, obtained using the discrete ordinates transport code DOT-IV (Rhoades et al., 1979). For a point source 15m above the air-ground interface, the above importance function was obtained for several mono-energetic neutrons ≤ 400 MeV, at few average radial distances ($\bar{r}$) of 11m, 108m, 495m and 1005m (with the source at radius of 0.0m) and for source cosine intervals of 1 to 0.8, 0.8 to 0.6, 0.6 to 0.4, 0.4 to 0.2 and 0.2 to 0.0.

For a given arbitrary neutron source $S(E, \cos\theta)$, neutron skyshine at the above average radial distances can be calculated using the neutron importance functions as given above. If the secondary gamma's produced and their energy distribution is known, then using similar photon importance function, gamma skyshine can also be calculated. Total skyshine component can be obtained by adding both the neutron and gamma components. The present method was tested with the experimental results of the Brookhaven alternating gradient synchrotron. The results were shown to give good agreement with the experimental data (Alsmiller et al., 1981), but the predictions differ from the experiment on an absolute basis by a factor of 2.5. The neutron skyshine dose calculated with the importance functions when used with the

Nakamura's (Nakamura et al., 1981b) experimental data found to agree with the measured values. With this method, neutron skyshine can be calculated only at four distances and hence for an arbitrary distance, one has to perform some sort of interpolation.

2.5 Monte Carlo simulation of neutron skyshine

In this, a brief review of Monte Carlo calculations on radiation transport at an air-ground interface has been attempted. Detailed calculations using the Monte Carlo technique have been done over the years (Trubey and comolander 1971, Ladu et al., 1968; Nakamura and Kosako, 1981a ; Hayashi and Nakamura, 1985). Ladu et al., (Ladu et al., 1968) have carried out Monte Carlo calculations for an isotropic point source of 5 MeV neutrons at an air-earth interface. They also studied the influence of lateral shielding by performing the calculations for different values of solid angles subtended upward by the source, $W = 2\pi(1 - \cos\theta)$. Values of θ chosen were $30^0, 60^0$, and 90^0. The first two cases correspond to accelerators without roof shielding but with thick lateral shielding and the last case corresponds to no shielding. Ladu et al., (Ladu et al., 1968) obtained empirical fit for these three cases and for different range of distances r from the neutron source.

$$\phi(r) = A\, r^{-\alpha} \quad 20\text{m} \leq r \leq 300\text{m}$$
$$\phi(r) = B\exp(-r/\lambda) \quad r \geq 300\text{m} \tag{2.4}$$

values of α and λ were found to depend somewhat upon the values of θ, but α was in the range of 1.5 to 1.6; and λ in the range of 200m to 300m. These results were found to agree with Lindenbaum's Eq. 2.1 but limited to $\approx$ few MeV neutrons whose behaviour was understood during the investigations of weapon's radiation effects, for the design of shielding in nuclear powered aircraft. Also Monte Carlo calculations were carried out for a fission neutron source, and upto energies of 14 MeV. Though they simulated the problem very close to reality, these calculations are very expensive

in terms of computer time and technique and therefore are inappropriate for a quick and detailed study of the variation of skyshine dose with respect to roof thickness, source spectrum etc.,.

2.6 Nakamura's formulation of neutron skyshine

A systematic study on neutron skyshine from nuclear facilities was carried out by Nakamura and his group (Nakamura and Kosako, 1981a; Hayashi and Nakamura, 1985). First a Monte Carlo analysis of neutron propagation in the air-over-ground environment from several mono-energetic sources was carried out. The neutron source was assumed to be in two conditions, one as a point isotropic cone, and other as a velocity collimated beam, both of these are fixed on the ground. A modified version of MORSE (Straker et al., 1970) called MMCR (Nakamura and Kosako, 1981a) a fast multigroup Monte Carlo code for cylindrical geometry has been used for the theoretical calculations. Calculations have been carried out upto ≈ 2 Km for several mono-energetic neutrons in the range of thermal to 14 MeV and for different source aperture angles between 0^0 to 85^0. The calculated total neutron flux $\phi(r)$ and dose $D(r)$ at a distance r from a source are well represented by a simple formula,

$$
\phi(r) = \frac{Q_\phi \ \exp(-r/\lambda_\phi)}{r}
$$
$$
D(r) = \frac{Q_D \ \exp(-r/\lambda_D)}{r} \tag{2.5}
$$

the constants $Q_\phi, \lambda_\phi, Q_D, \lambda_D$ are only dependent on the source neutron energy. There is little dependence of these constants on the upward aperture θ_S of the cone source. The Eq. 2.5 was tested at a fission, fusion and an accelerator facility, where in neutron skyshine dose was experimentally measured upto few hundred meters using rem counter. The following sections describe briefly the neutron skyshine studies carried out by Nakamura group at different nuclear facilities.

2.6.1 Skyshine from a fast neutron source reactor facility

The fission neutrons were extracted from the reactor core through a 60 cm diameter vertical hole penetrating the core assembly and the building wall; and hence the opening angle size was θ_S =2.5^0. The source neutron spectrum is measured with a proton recoil proportional counter and He^3 counter. Using the empirical formula given in Eq. 2.5, neutron skyshine dose was calculated and the results are in good agreement with the measured values (Nakamura et al., 1981b). About ±20% discrepancy was observed between 100 - 650m, but for ≤ 100m the calculated results give 50 - 100 % overestimation and this is due to the overestimation in the theoretical Monte Carlo calculation. Since, the coefficients Q and λ in the Eq. 2.5 were obtained using the empirical fitting of the calculated values, the error gets creeping in.

2.6.2 Skyshine from a 14 MeV intense source facility

The 14 MeV neutrons were generated from the deuterium-tritium(D-T) reaction. The absolute neutron source at the target is measured experimentally. The dose calculation with the Eq. 2.5 was performed, and is found to agree with the experimentally measured neutron skyshine dose using the rem counter (Nakamura et al., 1985). Tall buildings and a nearby hill are found to depress the skyshine effect and lower doses obtained nearby these points could not be explained.

2.6.3 Skyshine from the Electron Synchrotron

The skyshine neutron spectrum $S(E, \theta)$ leaked from the outer surface of the Electron Synchrotron was estimated with the DOT3.5 (Rhodes and Mynatt, 1973) code. The electrons were accelerated upto 650 MeV and were dispersed into the iron yoke magnet, are the projectiles generating source neutrons by undergoing photo-nuclear interactions. The source of the skyshine is the leakage neutrons from the upper shield surface, and was estimated using DOT3.5 in a two dimensional $r - z$ geometry. Calculation with the empirical formula Eq. 2.5 found to agree with the measured skyshine data (Nakamura and Hayashi, 1983) using rem counters within 30% beyond

1000m. The contribution of high energy neutrons i.e. > 14 MeV is found to increase with the distance and is about $\approx$ 60% of the total neutron skyshine dose. This shows that neutrons of energy > 14 MeV will contribute more than $\approx$ 60%. In section 5 we have shown theoretically obtained values of this factor at various distances. We observed that at large distances the contribution is almost 100%. Section 5 explains these facts with more details.

2.6.4 Extension of the Nakamura's formula to higher energies

As described earlier in the section 2.5 and the above subsections of 2.6, Monte Carlo calculations using a modified version of MORSE (Straker et al., 1970), MMCR (Nakamura and Kosako, 1981a) a fast multigroup albedo Monte Carlo code is found to agree with the experimentally measured skyshine phenomena at different nuclear facilities like, fission, fusion and accelerator. These results were extended from 14 MeV to 400 MeV using a new set of cross-sections HILO (Alsmiller and Barish, 1981). Albedo data of the ground to calculate the contribution of scattering from ground known as ground shine is considered. Skyshine of the secondary gamma rays was also analysed and is of the same form as neutron skyshine. The neutron emission angles from a cone source were fixed at five polar angles to estimate the angular dependence of the skyshine effect. The calculated neutron and secondary gamma-ray dose distribution were well fitted to the simple empirical formula at distances of 100m to 2000m from a source fixed at 0.0m or 15m above ground. The neutron skyshine dose at a distance of rm from the accelerator $D(r)$ is given by (Hayashi and Nakamura, 1985)

$$D(r) = \sum_i \sum_j \frac{Q(E_i, \theta_j)}{r} \exp\left[-r/\lambda(E_i, \theta_j)\right] S(E_i, \theta_j) \qquad (2.6)$$

Q, λ were obtained from the thermal to 400 MeV in 66 neutron groups. $S(E, \theta)$ is the leakage neutron skyshine source. This formula is tested with all the above nuclear facilities described and is found to reproduce all the experimentally measured values. The present work is based on this formulation to calculate neutron skyshine dose from particle accelerators.

2.6.5 Three-dimensional neutron skyshine measurements

For the first time three-dimensional neutron skyshine was measured by Nakamura's group (Uwamino and Nakamura, 1987) at the 1-GeV electron synchrotron, INS, Tokyo, Japan using a high-sensitivity dose-equivalent counter. It is found that the Eq. 2.6 represents the measured data very well. The source neutron spectrum as well as the actual skyshine source spectrum, which is nothing but the leakage neutron spectrum at the surface of the electron synchrotron building, was also measured experimentally. Further neutron skyshine transport calculations were performed using MMCR and DOT3.5. The calculated neutron spectra with these codes agreed well with the measured data and finally with the empirical formula Eq. 2.6.

2.7 Stevenson's survey of empirical formulae

Stevenson and Thomas (Stevenson and Thomas, 1984) based on his review work for the estimation of neutron skyshine, concluded that the empirical relation

$$\phi(r) = \frac{Q \exp(-r/\lambda)}{4\pi r^2} \tag{2.7}$$

is an adequate and simple expression for the neutron skyshine flux. He derived the values for Q and λ for proton accelerators and finally obtained

$$H(r) = 3 \times 10^{-13} \exp(-r/\lambda)/r^2 \quad \text{Sv/neutron} \tag{2.8}$$

where r is the distance from the accelerator measured in meters. For proton accelerators he made two simplifying assumptions.

- Neutron spectrum follows $1/E$ form up to the maximum energy of the accelerated proton.

- Neutrons are emitted into a cone whose semivertical angle is about $70^0 - 80^0$. This approximation may overestimate the dose-equivalent at large distances upto a factor of three, for sources which emit into a cone of very small vertical angles.

He also compared his method with Alsmiller et al., (Alsmiller et al., 1981) and Nakamura and Kosako (Nakamura and Kosako, 1981a) and found to agree reasonably well for all practical Health Physics purposes (a factor of 2 or ±50% uncertainty is allowed). Stevenson based on his review work tried to derive a recipe for neutron skyshine problem for the desk top calculations. Because of the available experimental and theoretical studies at proton accelerators, he finally settled down with an empirical formula for proton accelerators. The applicability of this method for other neutron environments is not tested.

2.8   Our method of calculation

Several empirical formulae exist for the neutron skyshine dose as described in the previous review at a distance from the source (Rindi and Thomas, 1975; Stevenson and Thomas, 1984; Hayashi and Nakamura, 1985). Among the different formulations, discussed in the previous review, Nakamura's formulation is widely tested in the different neutron environments. Also the empirical coefficients are energy dependent, and hence are more detailed. **Nakamura group's work is the single most authoritative research on the neutron skyshine phenomena.** This prompted us to select Nakamura's formulation for the neutron skyshine calculation. Hereafter the empirical formulation of Nakamura refers to the equation Eq. 2.9.

According to this formulation, the neutron dose $D(r)$ at a distance r from the source is given by

$$D(r) = \sum_i D(r, E_i) = \sum_i \left[\frac{Q(E_i)}{r} \exp\left(\frac{-r}{\lambda(E_i)S(E_i,t)}\right) \right] \qquad (2.9)$$

where $S(E_i, t)$ is the number of neutrons transmitted through the roof shield of thickness t with energy E_i, $\lambda(E_i)$ is the dose attenuation length of air for neutrons of energy E_i and

$$Q(E_i) = \lim_{r \to 0}[r \, D(r, E_i)] \qquad (2.10)$$

The parameters $\lambda(E_i)$ and $Q(E_i)$ are obtained using least-square fit to experi-

mental as well as calculated (Monte Carlo) data. These two parameters are found to depend on the neutron emission angle, i.e., the angle subtended by the roof to the neutron source. Both λ and Q are found to be slowly varying functions of energy. The value of Q varies between 2.79×10^{-11} and 6.77×10^{-12} μSv.meter. neutron and that of λ between 4.08×10^{-2} and 1.66×10^{-2}m for neutron energies from thermal (0.025 eV) to 400 MeV when r is expressed in meter and $D(r)$ in μSv.

The main advantage of such fitted expression is that they can approach the accuracy of the experimental data used for fitting while giving improved extrapolability which is required for the present investigations. Hayashi and Nakamura (Hayashi and Nakamura, 1985) has used this expression to benchmark problems of neutron skyshine from a fast neutron reactor facility, a 14 MeV neutron source facility and an electron synchrotron. The agreement between measured skyshine dose rates, and calculated with the Eq. 2.9 in all these cases was found to be good.

Hayashi and Nakamura (Hayashi and Nakamura, 1985) have tabulated the values of Q and λ for 10 energy groups and 5 source emission angle groups. These were estimated using the least-square fitting technique using the data calculated with a fast multigroup albedo Monte Carlo code. The code takes into account albedo data to estimate the scattering effect from the ground, the so called **ground shine** effect. The density of air was taken to be 1.2×10^{-3}g/cm^3 (1 atm, 20° C) and its composition : oxygen (1.05×10^{09} atom/cm^3) and nitrogen(3.96×10^{19} atom/cm^3). The density of the soil was taken to be 1.8 g/cm^3 containing SiO$_2$ and H$_2$O (5% by weight). The soil composition is hydrogen (6.02×10^{21} atom/cm^3), oxygen (3.73×10^{22} atom/cm^3) and silicon (1.72×10^{22} atom/cm^3). The results presented in this work is for the above air and ground conditions.

The number of neutrons transmitted through the roof shield of thickness t, $S(E_i, t)$, is obtained by multiplying the number of neutrons of energy E$_i$ falling on the inner surface of the roof of thickness t with the dose transmission coefficient $T(E_i, t)$, and then dividing by the flux to dose conversion factors, $f(E_i)$, ICRP60 (ICRP60, 1990) for neutrons. In our work, the dose transmission coefficient, $T(E_i, t)$ is based on either the neutron transport results of ASFIT or NCRP-51 (NCRP re-

port 51, 1977) recommended values. These details are described with more details in the section 3.3. The no. of transmitted neutrons $S(E_i, t)$ is given by

$$S(E_i, t) = \int_{\theta_{min}}^{\theta_{max}} \frac{\phi(E_i, \theta) T(E_i, t)}{f(E_i)} \tag{2.11}$$

where $\phi(E_i, \theta)$ is the number of neutrons with energy E_i emitted at an angle θ with respect to the direction of the accelerated ions, $(\theta_{max} - \theta_{min})$ gives the total angle subtended by the roof to the neutron emission point. All these factors Q, λ, T and ϕ were obtained at the intermediate energies by piece-wise exponential interpolations. To obtain the number of neutrons falling on the roof shield with energy E_i, we have to get the energy and angular distribution of neutrons, $\phi(E_i, \theta)$ coming out of targets bombarded with accelerated charged particles. These can either be measured or calculated using appropriate reaction model algorithms. We have experimentally measured and also theoretically calculated these neutron distributions. The calculations are based on the exciton model for pre-equilibrium emissions and the Weisskopf-Ewing calculations for compound nuclear evaporation. These are described with more details in sections 3.1 and 3.2.

2.8.1 Computer program for the calculation of neutron skyshine

A computer program in FORTRAN-77 is written for the calculation of the neutron skyshine dose using the algorithm described above. The program was compiled with a ND-560 Sintran operating system, FORTRAN-77 compiler. The program is also ported to a personal computer PC/486 and compiled with PC-based compilers. First the standard input parameters like the thickness of the proposed cyclotron roof, the source neutron distribution at some minimum four angles and other parameters were read. The program assumes a standard geometry of the roof for example the roof of K=130 Cyclotron VECC (Chatterjee and Muthukrishnan, 1982) which consists of 34 × 10 slabs (total 340 slabs) made of concrete of known composition. Then the respective dose-transmission kernels for the shield material were read from the input file. Now for each slab (whose dimension are given as parameters) the angle subtended with respect to the source (for example source is assumed to be the neutron

spectrum produced when 50 MeV alphas dumped on a Faraday Cup FC-01, a beam stopper for monitoring beam) is determined. Now the source neutron spectra for this angle has to be obtained by interpolation of the input source neutron spectra. A least-square fitting interpolation is found to give negative fluxes. So we have used the standard Legendre's (Kalbach-Mann systematics, 1981; kalbach, 1988) interpolation procedure. Legendre's expansion technique of the angular distribution is as old as neutron transport, and is also commonly used for such an expansion in many nuclear model calculations for the simulation of the emisstted neutron spectrum.

After obtaining the source neutron spectrum, the neutron skyshine source which is nothing but the leakage neutron spectrum, can be obtained by using the NCRP-51 recommended kernels or a detailed neutron transport. Our aim is develop a simple algorithm for a quick calculation of neutron skyshine dose. At this stage the neutron skyshine dose which has leaked from a given thickness of roof is available, and neutron skyshine dose at other distances can calculated using Eq. 2.9. The summation is done over all neutron energies and all the angles subtended by all the slabs with respect to the source.
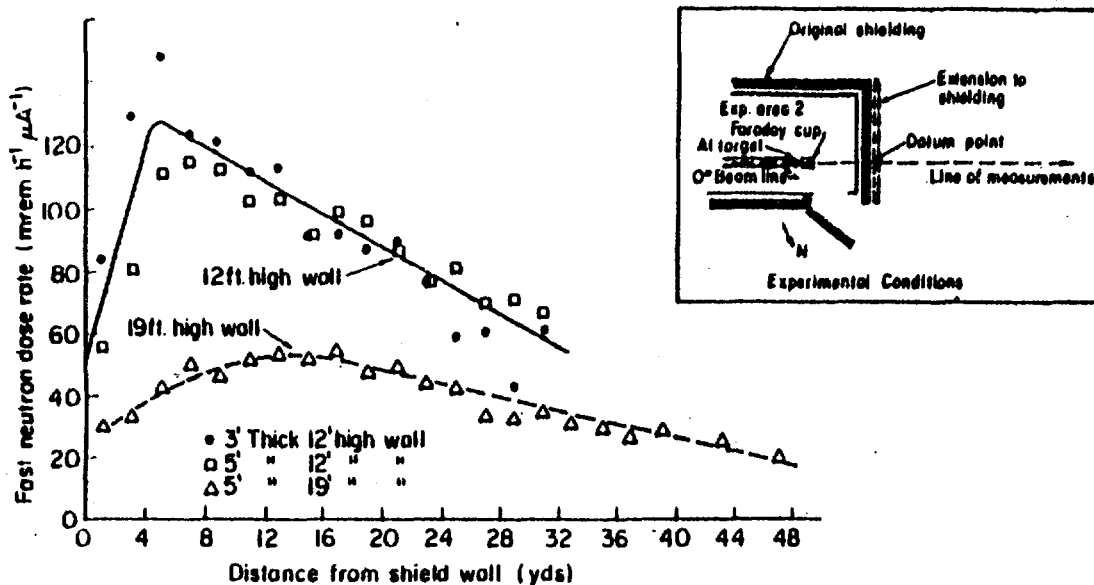
FIGURE 2.1 The variation of neutron dose rates as a function of distance from the 50-MeV proton linear accelerator of the Rutherford Laboratory. The inset shows the experimental arrangement. The upper (solid) curve is drawn through data points obtained with the original concrete shielding wall 12 ft high (3.65 m) and 3 ft (0.9 m) thick ($\odot$) and with an additional shielding added to give a total thickness of 5 ft (1.5 m) ($\square$) but with the same height. The dashed line is drawn through points measured with a concrete wall 19 ft (5.8 m) high and 5 ft (1.5 m) thick ($\triangle$).

3 Source Neutron Spectra And Neutron Transport

In order to estimate neutron skyshine dose one needs neutron spectra $\phi(E, \theta)$ emitted during the projectile-target interaction in the accelerator. To obtain the number of neutrons falling on the roof shield with energy E, we have to get the energy and angular distribution of neutrons, $\phi(E, \theta)$ emitted from targets bombarded with accelerated charged particles. These can either be measured or calculated using appropriate nuclear reaction model algorithms. We have experimentally measured and also theoretically calculated these neutron distributions. The calculations are based on the exciton/hybrid model for pre-equilibrium emissions and the Weisskopf-Ewing calculations for compound nuclear evaporation.

In this section the experimental measurement and theoretical calculations carried out at our laboratory is described. Also a one-dimensional neutron transport code for the treatment of neutron transport is described.

3.1 Experimental measurement of neutron spectra

Neutron spectra can be measured using several detector systems like He^3, NE-213, Bonner spheres, Threshold detectors using activation technique, solid state nuclear track detector CR-39, etc.,. Measurement of neutron spectra is very essential in view of the following :

- Benchmarking of neutron transport calculations.

- Shielding design considerations.

- Validation of neutron spectra calculated using nuclear model calculations.

In our laboratory we have measured neutron spectra using both NE-213, and Threshold detector activation technique for several projectile-target combinations using the charged particle beams from the VECC cyclotron. These details are discussed in detail in subsequent sections.

3.1.1 Neutron spectrometry using NE-213

Measurement of neutron spectra in a nuclear facility depends on several factors like energy range, flux and competing radiation's like gamma radiation etc.,. In an accelerator environment where neutron energy and flux can be dynamically controlled by the beam parameters, neutron detection using organic scintillators is the most convenient method. Plastic scintillators are having more limitations compared with liquid scintillators and NE-213 liquid scintillator is the most commonly used detector all over the accelerator community. The neutron field in general is always mixed with neutrons and gamma's. The pulse shape characteristics of these radiation's differ in a significant manner, and by exploiting this technique the gamma's are discriminated either on-line (during the experiment) or off-line (during an off-line analysis using computer software). The neutron spectrum is obtained by unfolding the measured light output from the scintillator. The limitations of this system are:

- The low energy threshold which is ideally about 0.5 MeV.

- gamma field should not be more than 10-20 mR/h.

In our lab we measured neutron spectra produced during 40-60 MeV alpha's on several targets *Be, Al, Ta, Au, Si, Ti* etc.,. We also measured neutron spectra for 15-30 MeV protons on *Ta, Al* targets. We have used in our laboratory, FERDOR a computer code for unfolding the measured light output using Monte Carlo calculated response functions, to obtain the neutron spectrum.

3.1.2 Neutron spectrometry using threshold detectors

Neutron flux determination using threshold detectors *Al, Au, In* is one of the oldest and routinely used technique. Neutron detection by threshold activation of several

foils is also used at high neutron flux facilities like nuclear reactor. This is also commonly used at high-energy accelerators as no other alternative exists to determine neutron spectra over several energy decades (typically 3-5 decades).

Neutron spectrometry can be carried out by selecting naturally abundant foils which have different threshold neutron energies. After a few hours of irradiation, the induced gamma activity of known gamma energy, can be measured with the HpGe semiconductor detector of known efficiency. The neutron spectra can be unfolded using known set of cross-sections. This unfolding is an underdetermined problem as with few gamma activity measurements several decades of neutron energy spectra has to be obtained. One of the great advantages of this technique is nearly infinite gamma rejection capability as compared to NE-213 detector, but requires high neutron flux. For reactor facilities where high neutron field is available, Multi Activation Detector (MAD) foils are available commercially, making this technique suitable for a routine survey of neutron flux. But in an accelerator environment neutron field is widely varying and so such facilities are not available.

In our lab we have measured neutron spectrum using this technique for 40-45 MeV α's incident on several targets like Be, C, and Ta. LOUHI is a general purpose unfolding computer program used for the determination of neutron spectrum from the measured induced gamma activity.

3.2 Calculation of thick target neutron yield

Neutron yield with a given projectile target parameters can be obtained using nuclear model calculations. Many of these models use simple phenomenological relations to detailed quantum mechanical schemes. The applicability of these models is widely varying over different energy ranges and types of projectiles, like for nucleon induced reactions, heavy ion induced reactions, etc., as the corresponding physics considerations are quite different. The physics for projectile energies < 250 MeV is different as for those above 250 MeV, as meson production needs to be considered. Nuclear Energy Agency (NEA), situated in France conducts inter-comparison studies between different models and their predictive capabilities for calculating neutron

20

yield required in several applications. Among the many available codes/schemes are PRECO-D2, ALICE91, GNASH, PEQAQ, EXIFON, HETC, LCS etc.,. Among these for a quick , reliable and general puipose estimation, codes PRECO-D2, AL-ICE91 were used in our laboratory.

In an accelerator environment neutrons are produced when projectiles (accelerated ions) hit different parts of the accelerator or the targets. The projectiles are completely stopped in that process. The source neutron distribution, $\phi(E_i, \theta)$ is, therefore, the energy and angular distribution of neutron yield from thick targets bombarded by charged particles. To calculate $\phi(E_i, \theta)$ we divide the thick target in a number of thin slabs, calculate the neutron yield distribution from each slab and then sum them to obtain the total yield spectrum. The thickness of each thin slab is so selected that the projectile loses ΔE_α MeV energy within each slab in a continuous slowing down process. We have ignored in our calculations the multiple scattering and straggling of emitted neutrons in the target. The effect of all these processes in the final neutron distribution is, we believe to be small. The kinetic energy of the projectile, E_α^j , incident on the j-th slab and the average energy, $\bar{E}^j{}_\alpha$, are given by

$$
\begin{aligned}
E_\alpha^j &= E_\alpha^0 - (j-1)\Delta E_\alpha \\
\bar{E}_\alpha^j &= \frac{E_\alpha^j + E_\alpha^{j-1}}{2}
\end{aligned}
\tag{3.12}
$$

The slab thickness x_j is

$$
x_j = \int_{E_\alpha^j}^{E_0} \frac{dE}{-dE/dx}
\tag{3.13}
$$

where $\frac{\Delta E}{\Delta x}$ is the α stopping power of the target material (Wiliamson et. al., 1966). The neutron yield $\phi(E_i, \theta)$ at energy E_α and direction θ to the beam axis is given by (Sarkar et. al., 1991)

$$
\phi(E_i, \theta) = \sum_{j=1}^{m} \sigma(\bar{E}_\alpha^j, E_i, \theta) N x_j \exp[-N(\sum_k \sigma_{abs}(\bar{E}_\alpha^k) x_k)]
\tag{3.14}
$$

21

where N is the target atomic density, $m = \frac{(E_\alpha^0 - E_\alpha^{th})}{\Delta E}$, E_α^{th} being the projectile threshold energy for neutron production. For $j = 1$ the value of the exponential attenuation factor in Eq. 3.3 is taken to be unity. Also we have,

$$\sigma_{abs}(\bar{E}_\alpha^k) = 2\pi \sum_i \int \sigma(\bar{E}_\alpha^k, E_i, \theta) \sin\theta d\theta$$

In the following two sections the nuclear models PRECO-D2 and ALICE91 are described for obtaining neutron emission cross-section for the given projectile-target combination.

3.2.1 Neutron yield calculation using PRECO-D2

PRECO-D2 (Kalbach, 1985) is a computer program written for calculation of nucleon emission cross-section for projectiles like nucleons, alpha's, and heavy ions but restricted to projectile energy less than 70 MeV. The calculations are based on the exciton model for pre-equilibrium nuclear reactions, and the standard Weiskoff-Ewing model for the evaporation or compound nuclear reactions. The angular distributions were obtained using Kalbach-Mann Systematics (Kalbach and Mann, 1981) which uses Legendre's expansion, whose coefficient's are expressed in the form of empirical relations connecting projectile-target parameters. We have modified this program to calculate thick target neutron yield using stopping power data. We have also included a new formalism (Kalbach, 1992) for the calculation of angular distribution using exponentials of cosine function which is not available in the standard distribution of the program. The mathematical formalism describing the formula for neutron yield is given in the following section.

Neutron yield expression for PRECO-D2

The double differential cross-sections $\sigma(\bar{E}_\alpha^j, E, \theta)$ are evaluated from the Kalbach-Mann systematics (Kalbach and Mann, 1981) that describes the angular distribution in terms of Legendre polynomials whose coefficients are given by simple phenomenological relations. For a given projectile energy $\bar{E}_\alpha^j$, the double differential cross-section

is

$$\sigma(\bar{E}_\alpha^j; E_i, \theta) = a_1(\bar{E}_\alpha^j, E_i) \sum_{l=0}^{lmax} b_l p_l(\cos\theta)$$

$$+ a_2(\bar{E}_\alpha^j, E_i) \sum_{l=0, \Delta l=2}^{lmax} b_l p_l(\cos\theta) \qquad (3.15)$$

where, $a_1(\bar{E}_\alpha^j, E_i) = (1/4\pi)\sigma_{pre}(\bar{E}_\alpha^j, E_i)$ and $a_2(\bar{E}_\alpha^j, E_i) = (1/4\pi)\sigma_{eq}(\bar{E}_\alpha^j, E_i)$ $\sigma_{pre}(\bar{E}_\alpha^j, E_i)$ and $\sigma_{eq}(\bar{E}_\alpha^j, E_i)$ are the cross sections for emission of neutrons with energy E_i for projectile energy $\bar{E}_\alpha^j$ from pre-equilibrium and equilibrium processes respectively. The coefficients b_l are functions of the neutron energy and are assumed to be of the form

$$b_l = \frac{(2l+1)}{1 + \exp[A_l(B_l - E - \beta)]} \qquad (3.16)$$

β being the neutron binding energy. The parameters A_l and B_l are free parameters and have been obtained in the Kalbach-Mann systematics by fitting with observed angular distributions as

$$A_l = [0.036 + 0.0039l(l+1)]$$
$$B_l = [98 - \frac{90}{(\sqrt{l(l+1)})}] \qquad (3.17)$$

In the code the cross-section $\sigma_{pre}(\bar{E}_\alpha^j, E_i)$ is evaluated using the exciton model and $\sigma_{eq}(\bar{E}_\alpha^j, E_i)$ by the Weisskopf-Ewing evaporation formula for compound nucleus equilibrium emissions. In the exciton model, the target projectile composite nucleus is assumed to reach compound nucleus equilibrium through a cascade of two-body interactions. Each stage of the binary cascade is characterized by the number of excited particles (p) and holes (h) termed as excitons. Emissions can take place from any stage of the binary cascade.

The pre-equilibrium differential cross-section is evaluated from the relation

$$\sigma_{pre}(\bar{E}_\alpha^j, E_i) = \sigma_{abs}(\bar{E}_\alpha^j) \sum_{p=p_0}^{\bar{p}} S_u(p) T_u(p) W_n(p, E_i) \tag{3.18}$$

where, $\sigma_{abs}(\bar{E}_\alpha^j)$ is the absorption cross-section of the projectile by the target, p_0 is the number particles excited at the first stage of the binary cascade giving rise to an initial exciton configuration (p_0, h_0) and $\bar{p}$ is the number of excited particles in the equilibrated compound nucleus. The summation over p ensures contributions from all stages of the cascade. $S_u(p)$ denotes the strength of formation of a configuration with p particles in the unbound stage, $T_u(p)$ is the mean life time of such a configuration, and $W_n(p, E_i)$ is the average rate for emitting a neutron with energy E_i and is given as

$$W_n(p, E_i) = \frac{2}{\pi^2 \hbar^3} E_i \sigma_n^{inv}(E_i) . dE Q_n(p) \frac{W(p-1, U)}{W^u(p, E')} \tag{3.19}$$

where $\sigma_n^{inv}(E_i)$ is the inverse cross-section, U and E' are excitation energy's of the residual and composite nuclei respectively and $W(p, E)$ is the density of states with p particles and excitation energy E, the superscript u refers to the unbound states. $Q_n(p)$ takes into account the neutron degrees of freedom assuming that in a two body interaction neutrons are excited in proportion to the densities of the configurations formed. In addition, two classes of direct reactions are included alongwith the pre-equilibrium cross-section. These are the nucleon transfer and nucleon Knockout reactions. These are evaluated semiempirically (Kalbach, 1985).

The energy differential equilibrium cross-section is given by

$$\sigma_{eq}(\bar{E}_\alpha^j, E_i) = [\sigma_{abs}(\bar{E}_\alpha^j) - \sigma_{pre}(\bar{E}_\alpha^j)] \frac{W_n(E_i)}{\sum_b \int W_b(E) dE_i} \tag{3.20}$$

where

$$W_b(E) = \frac{(2s_b + 1)}{\pi^2 \hbar^3} A_b E_i \sigma_b^{inv}(E_i) \frac{W(U)}{W(E)} \tag{3.21}$$

where A stands for the mass number and b indicates the type of particles emitted (e.g. for neutrons $b = n$) and s is the intrinsic spin of the ejectile. In the present case the state densities are assumed to be those for a single Fermi gas,

24

$W(E) \propto E^{-1} \exp(2(aE)^{0.5})$ and $a = (\pi^2 g_o)/6$ where in the present calculations we have considered the single particle level density, $g_o = (A/13)$

Now substituting Eq. 3.4 in Eq. 3.3 we get

$$\phi(E_i, \theta) = \sum_j (a_1(\bar{E}_\alpha^j, E_i) \sum_l b_l P_l \cos(\theta)$$
$$+ a_2(\bar{E}_\alpha^j, E_i) \sum_{l=0, \Delta l=2} b_l p_l \cos(\theta))$$
$$N x_j \exp([-N(\sum_k \sigma_{abs}(\bar{E}_\alpha^j) x_k)]$$
$$= a_1'(E_i) \sum_l b_l p_l \cos(\theta) + a_2'(E_i) \sum_{l=0, \Delta l=2} b_l p_l \cos(\theta) \qquad (3.22)$$

where

$$a_1'(E_i) = \sum_j a_1(\bar{E}_\alpha^j, E_i) N x_j \exp[-N(\sum_k \sigma_{abs}(\bar{E}_\alpha^k) x_k]$$
$$a_2'(E_i) = \sum_j a_2(\bar{E}_\alpha^j, E_i) N x_j \exp[-N(\sum_k \sigma_{abs}(\bar{E}_\alpha^j) x_k] \qquad (3.23)$$

In the present work we use Eq. 3.3-3.12 to calculate the angular distribution of neutron yield from thick targets. Eq. 3.12 is used to interpolate measured thick target neutron yield between emission angles where $a_1'(E_i)$ and $a_2'(E_i)$ are evaluated from the measured data using least-square fits.

3.2.2   Neutron yield calculation using ALICE91

ALICE91 (Blann M, 1991) is a computer program written in FORTRAN-77 for the calculation of emission of nucleons, deuterons, ^{3}H , He^3 for several projectiles including heavy ions. This differs from PRECO-D2 only in the treatment of pre-equilibrium nuclear reactions and employs hybrid/geometry dependent hybrid model for this purpose. Hybrid model is a modified form of exciton model where a never comeback approximation is used. Angular distribution can be obtained either using Kalbach-Mann systematics (Kalbach and Mann, 1981) or nucleon-nucleon kinemat-

ics. The mathematical formalism describing the formula for neutron yield is given in the following section.

Neutron yield expression for ALICE91

The Hybrid model calculates the pre-equilibrium(peq) energy spectra of nucleons only from the closed form expression, (Blann, 1991)

$$
\sigma_{peq}(\bar{E}_\alpha^j, E_i) = \pi \lambda^2 \sum_{l=0}^{\infty} (2l+1) T_l \sum_{\substack{n=n_0 \\ \Delta n=2}}^{\bar{n}} D_n
$$
$$
\times \left[X_n \frac{N_n(U, E_i)}{N_n(E)} \right] \frac{\lambda_c(E_i)}{\lambda_c(E_i) + \lambda_+(E_i)} \tag{3.24}
$$

Here, the subscript α denotes the projectile e.g., ^1H, ^6Li or ^{12}C and Where λ is the reduced de Broglie wave length of the projectile and T_l is the transmission coefficient of its lth partial wave. D_n is the depletion factor of the nth exciton state, (i.e., the probability of reaching the exciton state n without prior emission) and X_n is the number of excited neutrons in it. $N_n(E)$ is the number of ways in which the excitation energy E of the composite nucleus is shared among the n excitons and $N_n(U, E_i)$ is the number of ways in which the same energy E is distributed among n excitons with one particle exciton having the energy $E_i + B$ and the rest $(n-1)$ exciton sharing the energy $U = E - E_i - B$, B being the separation energy of neutrons, the ratio $N_n(U, E_i)/N_n(E)$ gives the probability of finding one neutron in the n-exciton state with energy $E_i + B$ prior to emission with energy E_i. The factor in the square bracket thus gives the number of neutrons with energy $E_i + B$ in the n-exciton state. $\lambda_c(E_i)$ is emission rate and $\lambda_+(E_i)$ is collision rate of nucleons with energy E_i. The hybrid model evaluates the pre-equilibrium spectrum under the "never come back approximation", i.e., each two-body interaction is assumed to always increase n to $n + 2$ by creating a particle-hole pair. The effect of annihilating a particle-hole pair is completely neglected in Eq. 3.13. This assumption is reasonably valid at the early stages of the nuclear relaxation process when the creation rate of a particle-hole pair is dominating over the annihilation rate but is certainly questionable at later stages

when this dominance no longer exists.

The energy differential equilibrium cross-section is given by

$$\sigma_{eq}(\bar{E}_\alpha^j; E_i) = [\sigma_{abs}(\bar{E}_\alpha^j) - \sigma_{peq}(\bar{E}_\alpha^j)] \frac{W_n(E_i)}{\sum_b \int W_b(E) dE_i} \qquad (3.25)$$

where

$$W_b(E) = \frac{(2s_b + 1)}{\pi^2 \hbar^3} A_b E_i \sigma_b^{inv}(E_i) \frac{W(U)}{W(E)} \qquad (3.26)$$

where A stands for the mass number and b indicates the type of particles emitted (e.g., for neutrons b = n) and s_b is the intrinsic spin of the ejectile. σ_b^{inv} is the inverse reaction cross-section of neutrons of energy E_i in the composite system. In the present case the state densities are assumed to be those for a single Fermi gas, $W(E) \propto E^{-1} \exp(2(cE)^{0.5})$ and $c = (\pi^2 g_o)/6$ where in the present calculations we have considered the single particle level density, $g_0 = (A/13)$.

The double differential cross-sections $\sigma(\bar{E}_\alpha^j, E, \theta)$ can be evaluated either by using semi-empirical systematics or by nucleon-nucleon kinematics. Kalbach-Mann systematics is a more commonly used method which (Kalbach and Mann, 1981) describe the angular distribution in terms of Legendre polynomials whose coefficients are given by simple phenomenological relations. A new version of these systematics (Kalbach, 1992) has also been used which describe the angular distribution in terms of exponentials using $cos(\theta)$ whose coefficients are also given by simple phenomenological relations. For a given projectile energy $\bar{E}_\alpha^j$,the double differential cross-section is

$$\sigma(\bar{E}_\alpha^j; E_i, \theta) = \frac{1}{4\pi} \sigma(\bar{E}_\alpha^j; E_i) \frac{a}{\sinh a} [\cosh(a\cos\theta) + f_{MSD}(E_i)\sinh(a\cos\theta)] \qquad (3.27)$$

where, the parameter a is the slope of the assumed exponential function and $f_{MSD}(E_i)$ is the ratio of pre-equilibrium cross-section to the total cross-section at the neutron emission energy E_i, as calculated using Hybrid model of Blann (Blann, 1991).

$$f_{MSD}(E_i) = \frac{\sigma_{peq}(\bar{E}_\alpha^j; E_i)}{\sigma(\bar{E}_\alpha^j; E_i)} \qquad (3.28)$$

where

$$\sigma(\bar{E}_\alpha^j; E_i) = \sigma_{peq}(\bar{E}_\alpha^j; E_i) + \sigma_{eq}(\bar{E}_\alpha^j; E_i) \qquad (3.29)$$

In the present work we use Eq. 3.13-3.18 to calculate the angular distribution of the neutron yield from thick targets. For this purpose we have modified the code ALICE91 (Blann, 1991), incorporating equations Eq. 3.13-3.18 in Eq. 3.3 to calculate the thick target neutron yield where from we estimate the values of a and f_{MSD}. In the code, the cross-section $\sigma_{peq}(\bar{E}_\alpha^j, E_i)$ is evaluated using the hybrid model and $\sigma_{eq}(\bar{E}_\alpha^j, E_i)$ by the Weisskopf-Ewing evaporation formula (Weisskopf and Ewing, 1940) for the compound nucleus equilibrium emissions.

Validation of ALICE91 with IAEA neutron yield

Comparisons have been made with the existing data, wherever available, with the results of the present calculations (Prabhakar Rao and Sarkar, 1997a). First, total neutron yield as calculated with ALICE91 code with the measured data as reported in IAEA Technical Report Series No. 283 (IAEA, 1988) for incident proton energies 10-100 MeV on thick Ta targets. Table 3.1 gives the comparison of total neutron yield as calculated by ALICE91 with the measured data of IAEA report for protons in the energy range between 10-100 MeV incident on thick Ta (ALICE91, 1991) and Cu (IAEA, 1988) targets. Though this comparison cannot be considered very exact, because of the non-availability of data for thick Ta targets assuming that this comparison will give some understanding of the neutron yield for thick targets. The difference between the yields in the above two cases is not significant which prompted us to carryout comparison of our present calculations (using Ta target) with those of IAEA data (using Cu target).

Table 3.1: Comparison of total neutron yield as calculated by ALICE91 with the measured data of IAEA report for protons in the energy range between 10-100 MeV incident on thick Ta (ALICE91) and Cu (IAEA) targets

Proton Energy (MeV)	ALICE91 (Blann, 1991) (1/proton)	IAEA (IAEA, 1988) (1/proton)
10	6.38E-5	2.00E-4
20	4.62E-3	2.40E-3
30	2.05E-2	2.00E-2
50	8.78E-2	6.60E-2
60	1.39E-1	1.20E-1
100	4.40E-1	3.40E-1

3.3 A brief review on neutron transport

The transmission of neutrons through different shield materials is the heart of neutron shielding design. At our laboratory we are making some efforts to develop computer methods for the shielding evaluation and participated in a benchmark (Nakane et. al., 1997) exercise conducted by NEA-JAERI. This subject field has grown enormously with the advent of Monte Carlo methods which inturn is due to the availability of cheap and high speed desktop computers. The complex three-dimensional geometry of any nuclear facility can be modeled using combinatorial geometry and shielding calculations can be performed using Monte Carlo codes like MCNP4A, LCS etc.,. Another popular and classical method of neutron transport is by discrete-ordinates. For this case only upto two-dimensional geometries can be implemented and any arbitrary geometries can't be modeled unlike Monte Carlo methods. In our lab a one-dimensional transport code ASFIT (Ramakrishna Rao, 1987) was developed for the treatment of neutron transport in the coupled neutron-gamma framework, and is described in detail in the following sections.

3.3.1 Neutron transport using ASFIT

The neutron transport through thick ordinary concrete slabs has been performed with ASFIT (Ramakrishna Rao , 1986 ; Prabhakar Rao and Sarkar, 1997a), a modified version of the original ASFIT-D (Gopinath and Santhanam, 1971) which was extensively used for the gamma transport. ASFIT-D is based on a semi-analytical technique for the solution of the transport equation in one-dimensional finite systems. The method is applicable to multi-energy, multi-region systems with arbitrary degree of anisotropy. The transport equation is written in the form of coupled integral equations separating the spatial and energy-angle transmissions. Legendre polynomial expansion in the direction cosine, and discrete ordinate representation in the energy and spatial domain are used for radiation source and flux. The space and energy-angle transmission kernels are evaluated analytically and the integral equations are then solved by a fast converging iterative technique. For a plane parallel beam of radiation incident on a slab shield, the virgin and the first collision flux are not amenable to polynomial expansion due to the singularities. For such a case, upto a second collision, source is computed analytically and then recourse is taken to polynomial expansion. Let an one-dimensional slab of a given medium be divided into n number of meshes of constant thickness $x_1, x_2, x_3 \ldots x_n$, and the source neutron spectrum $\phi(E_i, \theta)$ be regrouped into m energy and k direction cosines($\mu = \cos\theta$), as $\phi(E_g, \mu_i)$ where the group structure is according to the cross-section . Let the angular source be in terms of direction cosines $\mu_1, \mu_2 \ldots \mu_k$. The grouping of neutron yield according to the cross-section structure is explained in this following sub-section.

Grouping of neutron spectra according to cross-section

The input spectrum is generally given in a fixed bin structure, where as any discrete ordinates solution of the neutron transport requires the input spectrum to be of the same group structure as that of cross-section. The working principle for any grouping of spectra should be that, the total area should be same in the old as well as in the new group structure. Let $\phi(E_k)$ represent the input neutron yield and $\phi(E_g)$ is the new group to be obtained. First, the given spectra $\phi(E_k)$ is summed over to obtain

the cumulative spectrum $\Phi(E_k)$, and is given by,

$$\Phi(E_k) = \sum_k \phi(E_k)\Delta E_k$$

Then the cumulative spectra are linear interpolated to get $\Phi(E_g)$ over the new cross-section group structure. The required grouped spectra in the new group is obtained using the following equation

$$\phi(E_g) = \frac{(\Phi(E_g) - \Phi(E_{g-1}))}{\Delta E_g}$$

Mathematical formulation

The source and flux densities are represented by

$S(x_j, E_g, \mu_i)$ and $f(x_j, E_g, \mu_i)$ respectively, at the space point x_j for source neutrons of energy E_g, and direction cosine μ_i. Under equilibrium conditions

$$\phi(x_j, E_g, \mu_i) = \int S(x', E_g, \mu_i) \, T(E_g, \mu_i, x'_j \to x_g) \, dx' \tag{3.30}$$

and

$$S(x_j, E_g, \mu_i) = 2\pi \int \int \phi(x_j, E', \mu') \, G(x_j, E' \to E_g, \mu' \to \mu_i) \, dE' \, d\mu'$$
$$+ S'(x_j, E_g, \mu_i) \tag{3.31}$$

where $S'(x_j, E_g, \mu_i)$ is the non-scattering source, $T(E_g, \mu_i, x' \to x)$ and $G(x_j, E', \mu' \to \mu)$ represent, the transmission and the scattering kernels respectively. The spatial integral in Eq. 3.19 is evaluated by using the discrete ordinate representation in space and angle and is given by,

$$S(x, E, \mu) = \sum_{n=0}^{N} S_n(x, E) \, P_n(\mu)$$

$$\phi(x, E, \mu) = \sum_{n=0}^{N} \phi_n(x, E) \, P_n(\mu) \qquad (3.32)$$

Hence, Eq. 3.19 can be rewritten as

$$\phi(x_j, E_g, \mu_i) = \sum_{j'} \int_{x_{j'}}^{x_{j'+1}} S(x', E_g, \mu_i) \, T(x' \to x_j, E_g, \mu_i) \, dx' \qquad (3.33)$$

We can also write, interms of Legendre coefficients

$$\phi_n(x_j, E_g) = \frac{(2n+1)}{2} \sum_{u} \phi(x_j, E_g, \mu) \, P_n(\mu_i) \, W_i \qquad (3.34)$$

where W_i is the gaussian weight and μ_i the direction cosine. Legendre polynomial approximation of all the relevant quantities is then used to evaluate the collision integral over the angle. Eq 3.19 can be written as

$$S_n(x_j, E_g) = \sum_{g'} \int_{E_{g'}}^{E_{g+1}} \phi_n(x_g, E') \, G_n(x_j, E' \to E_g') \, dE' + S'(x_j, E_g, \mu_i) \qquad (3.35)$$

Where S_n and ϕ_n represent respectively the nth Legendre coefficient of the source and flux at the spatial point x_j and the energy E_g. To carryout the integration the energy in Eq. 3.24 the flux coefficients were linearly interpolated in energy between $E_{g'}$ and $E_{g'+1}$ at a given spatial node x_j.

Computational method in ASFIT

Based on the formulation described above a computer program in FORTRAN-77, ASFIT has been written for a plane parallel beam of mono or poly-energytic neutrons, incident normally on one-side of an oridnary concrete slab, finite in the x-direction and infinite in the lateral direction. The one-dimensional slab was mathematically divided into a number of meshes of constant mesh width which is chosen

as a fraction of the incident neutron mean free path. The uncollided transmitted fluxes at each mesh point is calculated analytically. These uncollided fluxes which generate first collision sources during their interaction with medium, were also calculated analytically. The iteration starts with the calculation of flux coefficients at all space and energy ordinates using the spatial transmission matrix and the available source coefficients. Next the source coefficients are recomputed from these fluxes and the collision matrix. This completes one iteration and the procedure is repeated until the source terms in successive iterations agree within a pre-set convergence criterion, an approximation of the equilibrium condition to satisfy the original assumption in the integral formulation. We have performed extensive studies to obtain the optimum parameters for the convergence with the number of iterations, angular convergence, mesh width, and for several mono-energetic neutrons with energies ranging from thermal to 400 MeV incident on ordinary concrete slabs made of TSF 5.5% (NCRP-51, 1977) composition (the composition of this concrete given in the units of 10^{21} atoms/cc is: hydrogen 8.50, carbon 20.20, oxygen 35.50 , aluminium 1.86, silicon 1.70, calcium 11.30, iron 0.19 and water by percent weight 5.5). To facilitate the spectrum transport, the incident spectra has been grouped according the HILO (Alsmiller and Barish, 1981) cross-section structure. For the calculation of dose due to neutrons and secondary gamma's, ICRP60 fluence to dose-conversion factors (ICRP60, 1990) were used. A recommended semi-log interpolation (Sims and Killough, 1983) scheme has been adopted for the interpolation of the intermediate energies, in order to calculate the dose for poly-energetic neutron spectrum.

Cross-section used in ASFIT

For our purposes we have chosen a 47 neutron, 15 gamma total 61 group to group cross-sections, DLC-58 / HELLO (Alsmiller and Barish, 1978) spanning thermal to 60 MeV neutron energies and gamma energies up to 15 MeV. The advantage of such cross-sections is its ready adaptability to our method of solution. These are the most commonly used set of cross-sections implemented in codes like ANISN, MORSE-CG etc.,. A later version of these cross-sections named HILO (Alsmiller

and Barish, 1981) was is also used for high energy neutron transport up to 400 MeV. This set consists of 66 neutron groups covering from thermal to 400 MeV and gamma's of the same range as HELLO since the contribution of gamma's to the total dose for energies more than 15 MeV is found to be insignificant (Roussin et. al., 1972). Using this set of cross-sections we have implemented coupled neutron - gamma transport making our code compatible with the other computer programs of radiation transport like ANISN, MORSE-CG.

As a validation for the above method in ASFIT we compared our calculations with IAEA and also the results were used for the shielding design of K-500 super conducting cyclotron. These details are given in the following section.

IAEA method of shield thickness calculation

IAEA (IAEA, 1988) has given transmitted dose through concrete for proton beam incident on thick Cu target, over a fairly wide range of shield thicknesses using simple equation of the from:

$$H(d, \theta) = r^{-2} \, H_\theta \, exp(-d(\theta)/\lambda_{eff}) \qquad (3.36)$$

where,

- $H(d, \theta)$ is the dose equivalent at depth d, angle θ in the shield;

- H_θ is a constant that may be descried as the dose equivalent extrapolated to zero depth in the shield, and corresponding to angle θ, and at unit distance from the point source ;

- r is the distance from the source to shield surface(or other point of interest outside the shield) ;

- λ_{eff} is the effective attenuation length for dose equivalent through the shield.

Experience has shown that, over a limited range of shield thicknesses, the approximation of the radiation transmission by an exponential function works well: it fails for shield thicknesses less than about 1000 kg/m^2. In principle, values of the

dose equivalent H as a function of both angle and depth are needed for shield design. However it is often only necessary in practice to design shielding in the longitudinal (or forward) $\theta = 0$ and transverse (or lateral) $\theta = \pi/2$ directions.

Validation of ASFIT with IAEA method

Figures 3.1 and 3.2 give the transmitted neutron dose through concrete both in the forward (0^0) and lateral (90^0) directions with respect to the proton beam of energies 50 and 100 MeV incident on thick Ta targets. The above figures give calculations using Eq. 3.25 (points) and those using our method (solid lines joining points). It is observed that the agreement in the forward direction is good whereas in the lateral direction IAEA results gives underprediction which increases with increasing concrete thickness. This discrepancy may be attributed to the difference in the angular distribution of the neutron spectra in the two calculations. With Eq. 3.25 we have used the following parameters.

For 50 MeV proton beam

$$H_0 = 1.40 \times 10^{-15}, \quad \lambda = 470(\text{kg/m}^2) \quad \text{for } \theta = 0^0$$

$$H_0 = 1.80 \times 10^{-16}, \quad \lambda = 320(\text{Kg/m}^2) \quad \text{for } \theta = 90^0$$

For 100 MeV proton beam

$$H_0 = 1.80 \times 10^{-15}, \quad \lambda = 770(\text{Kg/m}^2) \quad \text{for } \theta = 0^0$$

$$H_0 = 4.80 \times 10^{-16}, \quad \lambda = 460(\text{Kg/m}^2) \quad \text{for } \theta = 90^0$$

Figures 3.3 and 3.4 give the transmitted doses in the forward (0^0) and the lateral (90^0) directions for 150 MeV carbon and 500 MeV lithium, respectively, incident on thick Ta targets. The transmitted dose data of 500 MeV lithium is used for the shielding considerations of the K=500 superconducting cyclotron shield design (Health physics report, 1995). IAEA (IAEA, 1988) gives another parametrisation using exponential function in the following form,

$$H(d) = k_0 \, exp(-x/\lambda) = \sum_E K_0(E) \, exp(-x/\lambda(E)) \qquad (3.37)$$

Where $H(d)$ is the dose equivalent at depth d in the shield, x is thickness of the shied, λ is the attenuation length, and k_0 is the extrapolated dose equivalent at zero depth. IAEA (IAEA, 1988) given the values of k_0 and λ for neutron energies from 5-1000 MeV through concrete. We have used these values and the formula given by Eq. 3.26 to compare with our present calculations. In both the cases source neutron spectra calculated with ALICE91 were used. Results of our calculations (solid line joining points) and those using Eq. 3.26 (points) are shown in Figures 3.3 and 3.4. The agreement is good though there are some trends of increasing discrepancy at larger thicknesses. This can be attributed to the differences in the two calculation methods for neutron transport.

We have compared ASFIT calculations with the data given in NCRP-51 (Prabhakar Rao and Sarkar, 1997a) through ordinary concrete (TSF 5.5%) of several mono-energetic neutrons. Figure 3.5 gives the comparison for 100.0, 70.0, 33.0, 13.6 - MeV incident neutron energies for ASFIT calculations in comparison with NCRP-51 values. Difference in the energy group structure used in the above two calculations are responsible for the difference in incident energies used in the comparison. The agreement is good in this case also.

3.3.2 Neutron dose transmission kernel NCRP-51 method

Transmitted neutron dose for an incident neutron spectrum $\phi(E,\theta)$ can be obtained either by considering a detailed neutron transport or by using NCRP-51 dose transmission kernel. For a quick calculation of the required shield thickness, several organisations and laboratories use this kernel method. These transmission kernels are obtained after a rigorous and detailed transport calculations. The advantage of such a kernel is that with proper recommended interpolation or extrapolation methods, transmitted dose for arbitrary shield thicknesses or neutron energies can be easily obtained. NCRP, an American committee who has in their report **Radiation protection design guidelines for 0.1-100 MeV particle accelerator**

facilities have supplied the kernels in terms of graphs. Dose-equivalent transmission per unit-fluence (rem/cm^2) for mono-energetic neutrons incident on slabs of ordinary concrete (TSF5.5, 2.31 gm/cc (NCRP-51, 1977)) were given. Multi-collision dose-equivalent index per unit-fluence is calculated using ANISN (Roussin et. al., 1972) code including the c ontribution of capture gamma rays produced within the slab. We have compared this results with our calculation using ASFIT (Prabhakar Rao and Sarkar , 1997a) and the agreement is good (see Figure 3.5). In our program for the neutron skyshine calculation we provided an option to treat neutron transport either by ASFIT or NCRP-51 kernel.

3.3.3   K-500 shielding design using ASFIT

We have carriedout shielding design studies using ALICE91 + ASFIT code system for a new proposed K-500 super conducting cyclotron at Calcutta. We have compared the transmitted dose for different projectiles like 80 MeV proton, 150 MeV carbon, 500 MeV lithium (Prabhakar Rao and Sarkar, 1997a; Health Physics unit report, 1995). Figure 3.6 shows the transmitted dose equivalent for different thickness in Kg/m^2 made of ordinary concrete. These projectiles when incident on thick tantalum targets produce neutron spectra. The source neutron spectra is calculated using ALICE91 code. The transmitted neutron dose is calculated using ASFIT. The results are compared with the those obtained using NCRP-51 recommended values and the agreement is good. But NCRP-51 values are available only upto 600 gm/cm^2 (2.59 m) where as present shielding considerations require about 4 meters of thick concrete slabs. We had studied ASFIT and its applicability for deep penetration problems, and we found that ASFIT can be used upto 6.0 meters of ordinary concrete. Based on these studies shield recommendations were given and about 3.5 meter of ordinary concrete or equivalent is found to be the optimum thickness inside the cyclotron vault and 1.5 meter for the experimental caves (Health Physics Unit, 1995) for designing roof shields. The neutron skyshine dose was also estimated and the details are in section 4.
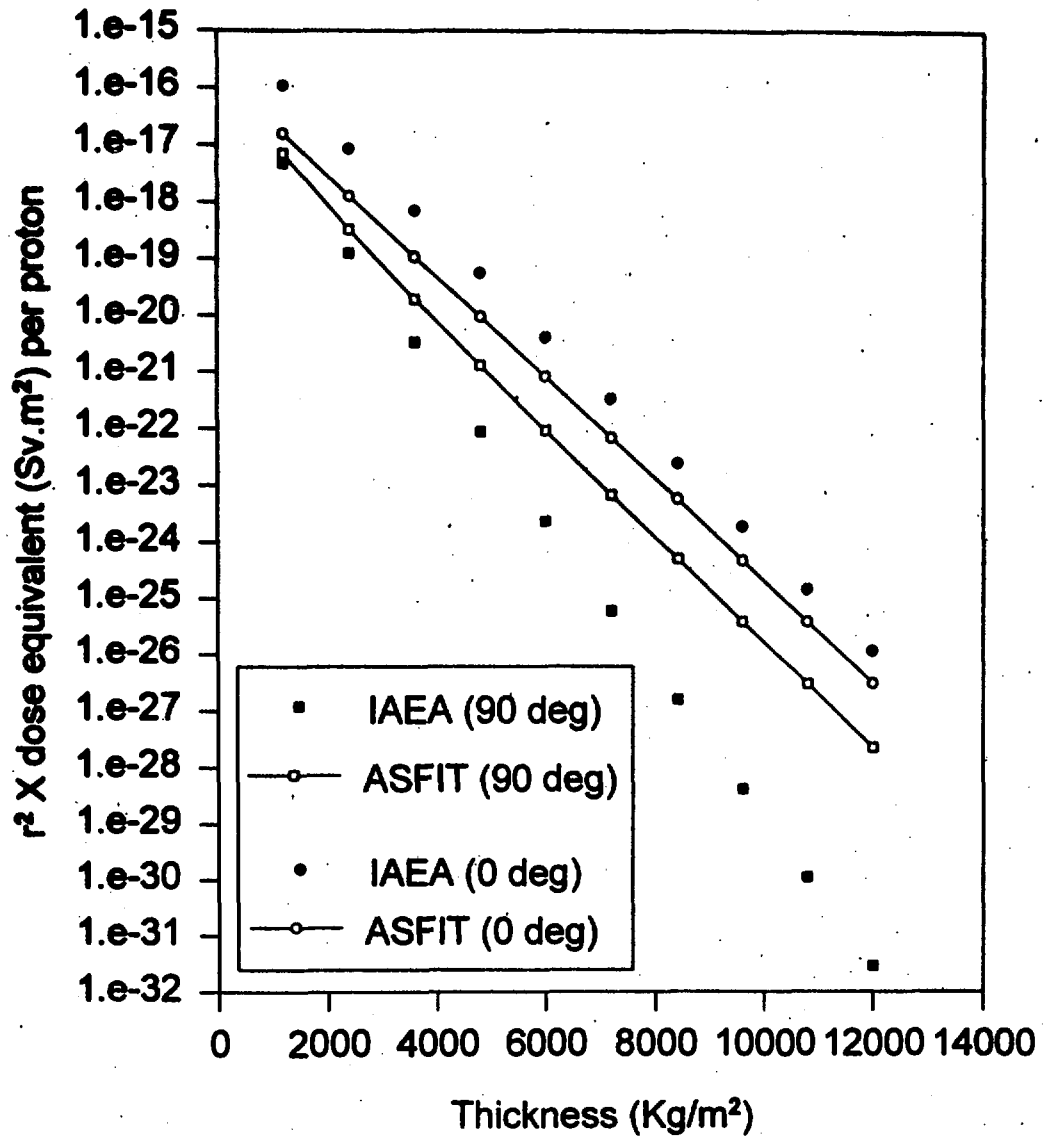
37

Figure 3.1: Comparison of transmitted dose equivalent as a function of depth in ordinary concrete for proton of energy 50 MeV incident on thick targets of Cu (IAEA) and Ta (ALICE91).
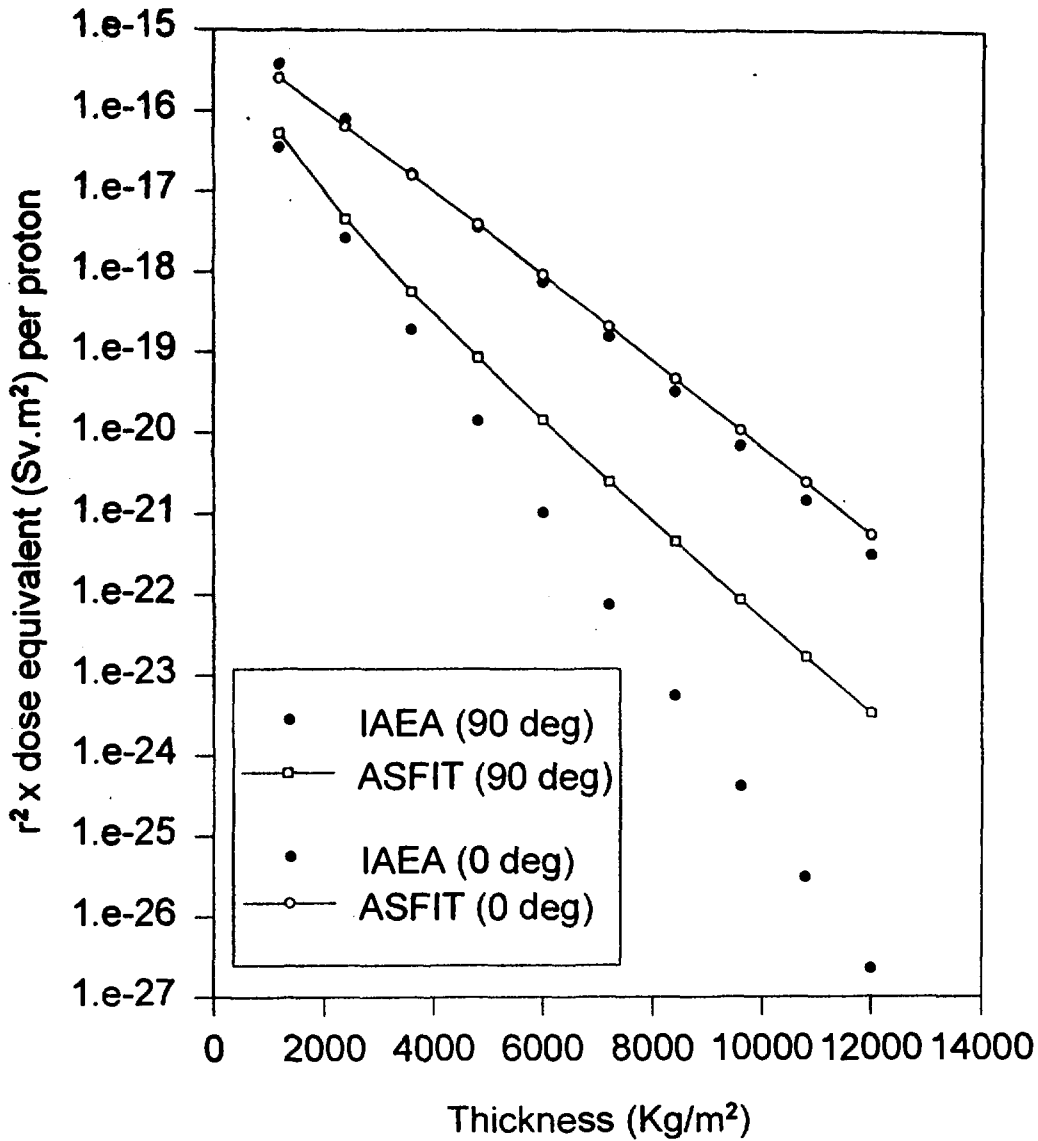
Figure 3.2: Comparison of transmitted dose equivalent as a function of depth in ordinary concrete for protons of energy 100 MeV incident on thick targets of Cu (IAEA) and Ta (ALICE91).
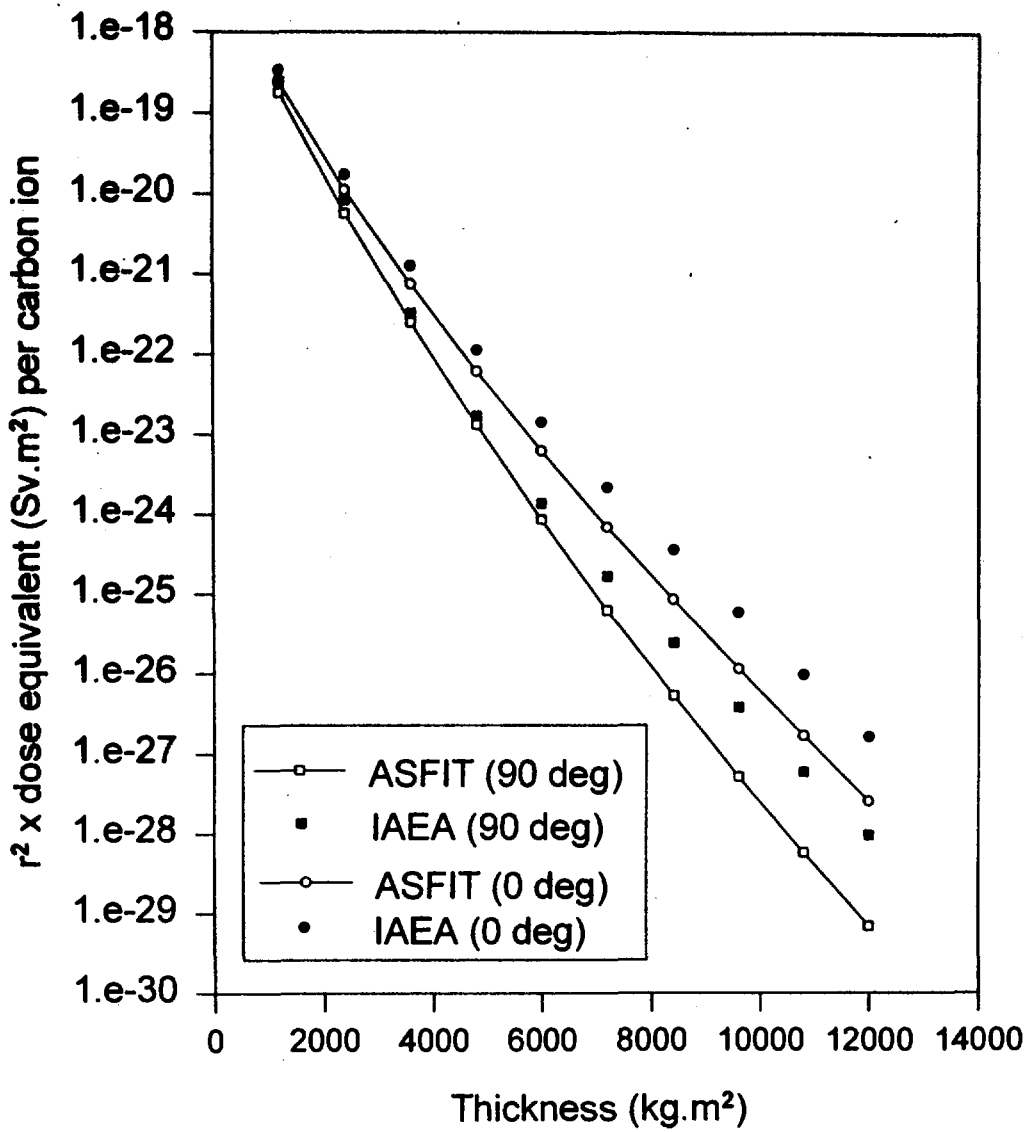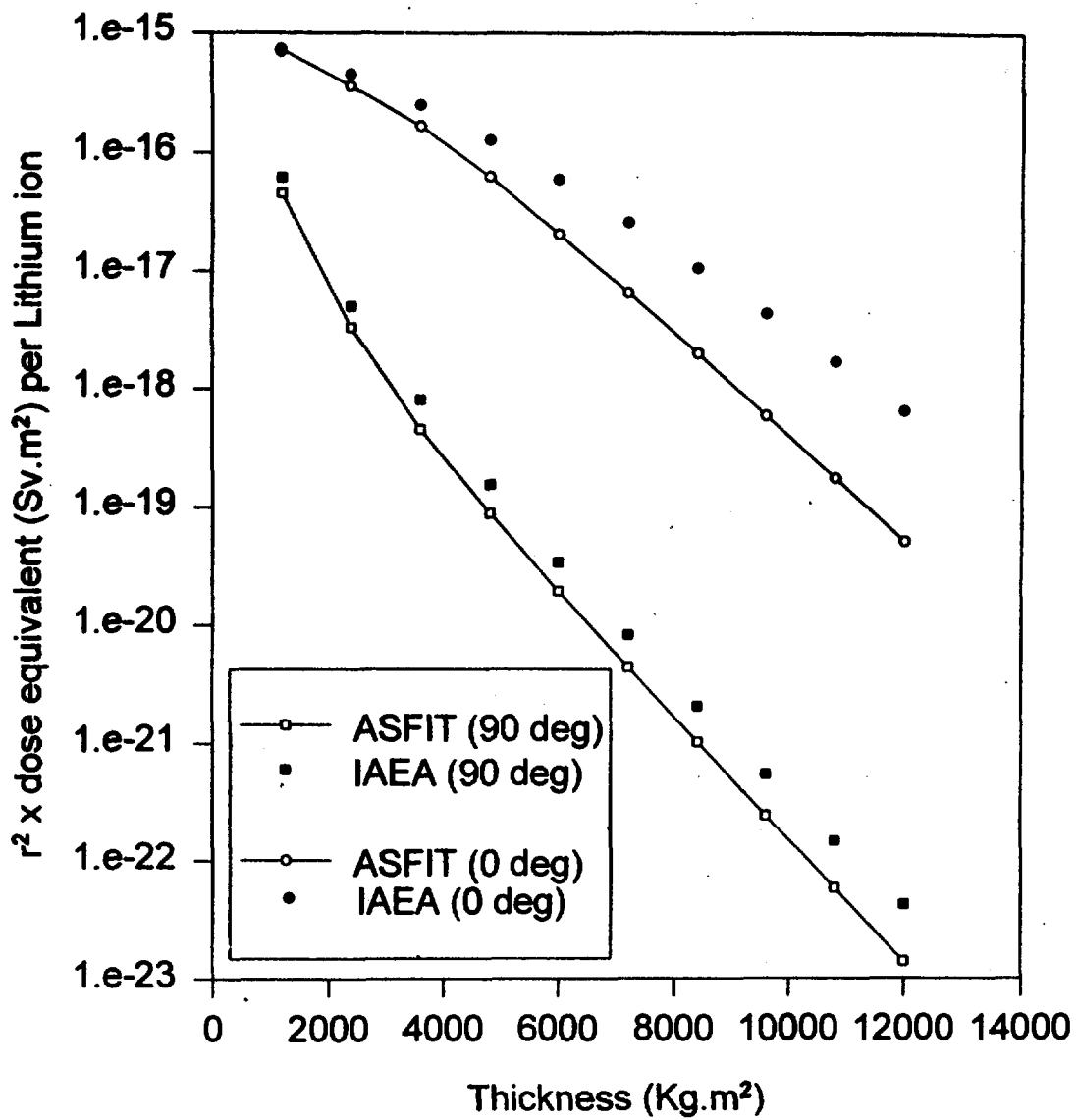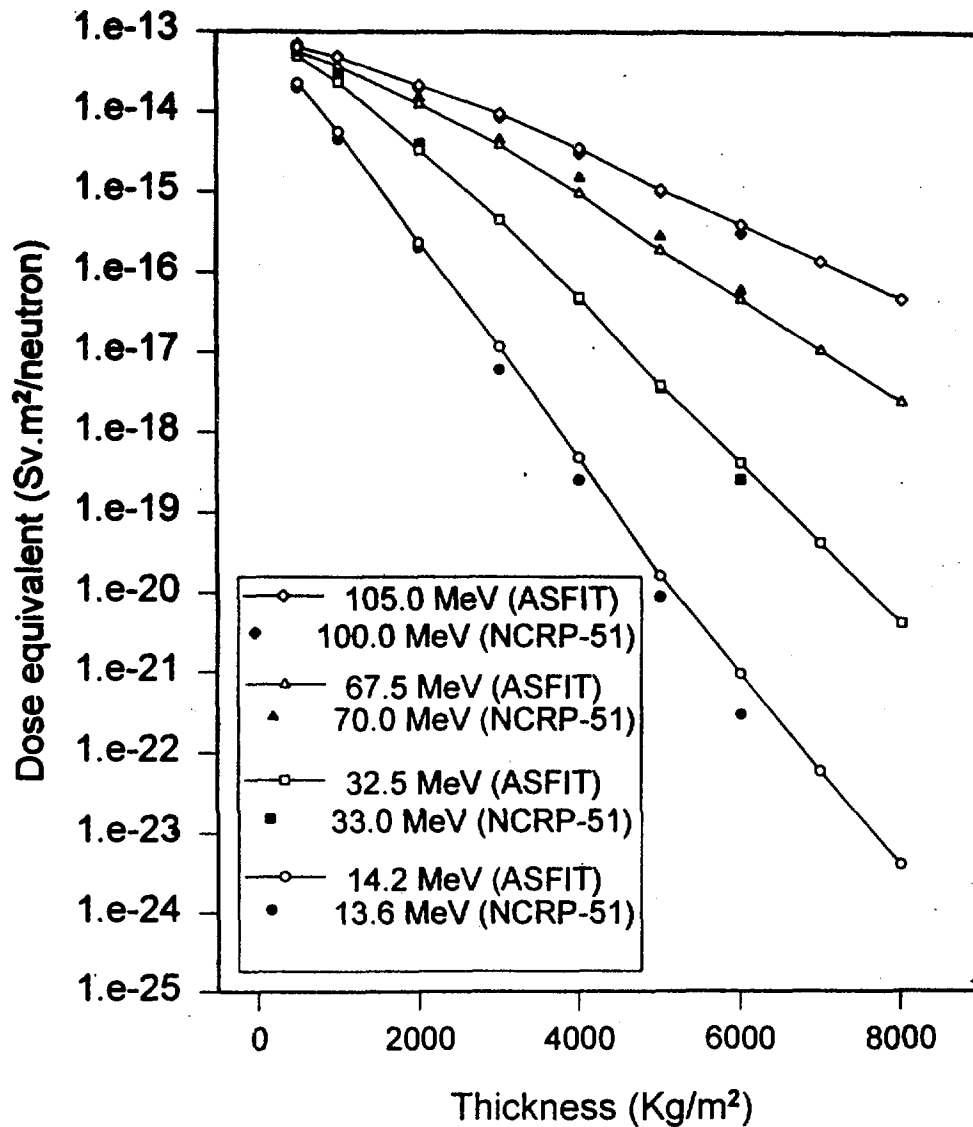
Figure 3.3: Comparison of transmitted dose equivalent
a function of depth in ordinary concrete for carbon
of energy 150 MeV incident on thick Ta target.

Figure 3.4: Comparison of transmitted dose equivalent as a function of depth in ordinary concrete for lithium of energy 500 MeV incident on thick Ta target.

41

Figure 3.5: Comparison of dose equivalent index of transmission per unit fluence (Sv.m^2) of mono-energetic neutrons incident normally on slabs of ordinary concrete (TSF5.5) as obtained using ASFIT and NCRP-51.
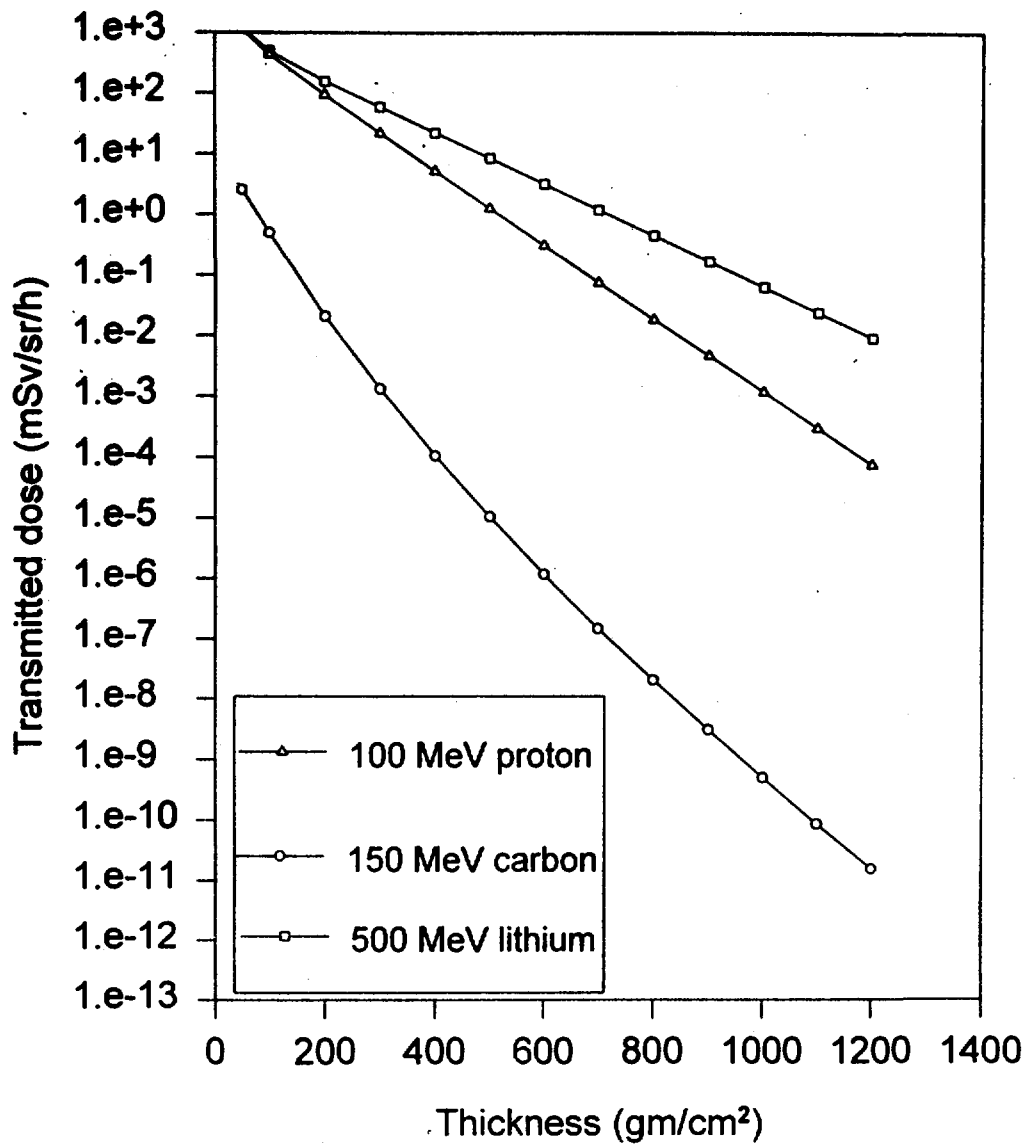
Figure 3.6: Comparison of transmitted dose equivalent for various ions obtained by performing neutron transport with ASFIT. The source neutron yields were obtained using ALICE91.

4 Application Of The Present Method For The Shielding Design

4.1 Neutron skyshine dose calculation for VECC.

VECC, is a K=130 variable energy cyclotron which can accelerate positively charged particles like alpha's upto 130 MeV , protons and deuterons upto 65 MeV. VECC, is an 84" cyclotron, and is adapted from Lawrence Berkeley Laboratory. Beam currents can be upto 10μA external and 100 μA internal. A new heavy ion source based on electron cyclotron resonance (ECR) will be installed in the later part of this year, using which heavy ion beams can be obtained.

We have calculated neutron skyshine using Eq. 2.9 as described in section 2. The source neutron spectra are obtained using PRECO-D2 for the given target projectile configuration, which is explained in section 3.2.1. We have also used experimentally measured neutron spectra using NE-213 organic scintillator. We considered 20 μA, 50 MeV alpha's incident on FC-01 (beam stopper) as the representative beam.

Based on the above formulations as described in section 2 and section 3, a computer code has been developed which estimates the neutron skyshine dose at various distances from the accelerator. The code takes into account the structural configuration of the VECC, especially its roof shield. The present roof shielding of VECC consists of a 36 × 10 matrix of concrete slabs with an average area of 0.92 square meters per slab arranged in two staggered layers of 0.8m and 0.7m thickness (total 1.5m) such that the edges of the concrete slabs placed one above the other will not be in the same vertical plane, thus preventing direct neutron leakage to outside. The code calculates neutron skyshine dose with the present shielding as well for configurations where any number of slabs from any position is removed including a complete removal of the roof shielding. Presently, the code considers the source of neutrons to be at the position of the Faraday cup, FC-01, inside the cyclotron vault.

Though the major beam loss and thus the most predominant source of cyclotron produced neutrons is at the septum, the neutron emissions at the septum is heavily shielded on top by the main magnet and was found to contribute insignificantly to the skyshine dose. With a slight modification of the code one can have the source distributed over a surface or a volume anywhere in the vault or in the experimental caves. Flux and total number of neutrons incident on the inner surface of the roof are calculated separately for each of the 36 × 10 individual slabs. An interpolation scheme based on Legendre polynomials is used to compute the number of neutrons per MeV per steradian at directions of the straight lines joining the midpoints of each slab and the source. The main aim of the present code-development is to keep the algorithm simple enough to be able to make quick and easy calculations with the help of personal computers for various combinations of the parameters like target material, projectile type and energy, beam current etc.

4.1.1 Results and discussion

We have considered the neutron spectrum produced when a 20 micro-ampere alpha beam is dumped on FC-01. The projectile energy considered is 50 MeV. We are interested in calculating the neutron skyshine dose rates at various distances from the source for the following configurations:

 (i) present VECC roof shielding;

 (ii) one slab removed from the position corresponding to the extreme forward angle with respect to the beam direction;

 (iii) same as (ii) but the slab position corresponds to the extreme backward angle;

 (iv) complete removal of the roof shielding.

Figure 4.1 gives the neutron skyshine dose rates (Prabhakar Rao and Sarkar, 1993b) at various distances with the present roof shielding for both measured and calculated neutron spectra. It is seen that at any distance the dose rate due to skyshine neutrons is much smaller than the natural background dose rate which is

45

0.1μ-Sv/h. In Figure 4.2 we have shown the neutron skyshine dose at various distances ranging from 100 to 2000m for extreme forward angle and extreme backward angle and also for both measured and calculated source neutron spectra. It is observed that the dose is more in forward direction than due to backward direction as is due to the large high energy component in the former case. Also the dose is more for measured spectra than the calculated one and is due to the underestimation of high energy component in the theoretical model (Sarkar et. al., 1991). In Figure 4.3 we give neutron skyshine dose when total roof shielding is completely removed. The calculated dose rate at 100m for the measured source neutron yield from the accelerator is 0.03653μ-Sv/h and that for calculated source neutron yield is 0.02757μ-Sv/h.

4.1.2 Conclusion

A simple algorithm for calculating neutron skyshine dose rate has been presented where the effectiveness of the present VECC overhead shielding has been confirmed. This same methodology can be used for proper shielding design to regulate the population dose.

4.2 Neutron skyshine dose calculation for K=500 cyclotron.

A new super-conducting cyclotron with K=500 is proposed at VECC, Calcutta. This cyclotron can deliver heavy ions beams with more energy than what VECC can afford and is the only such facility of its kind planned in INDIA. The shielding design (Brief report of Health Physics Unit, 1995) was carried out by our lab and some results are presented briefly in this report. The following projectile types and energies have been considered as the design parameters of the cyclotron.

Projectile	Energy	Expected beam current (pnA) at extraction radius
proton	80 MeV	100
^{7}Li	500 MeV	50

The Neutron skyshine dose due to air-scattered neutrons was calculated using the Eq. 2.9. The algorithm used in the above section while calculating the neutron skyshine dose was used. The geometry and other considerations are assumed to be to be similar to the VECC cyclotron. It was found that optimum roof over the vault is 2.0 m and over the experimental caves is 1.0 m of ordinary concrete. Figure 4.4 gives the dose-equivalent rates at various distances from the accelerator with and without roof shield for 500 MeV ^{7}Li beam (50 pnA at extraction radius). While recommending roof shielding, consideration was given to the fact that public residential areas start from about 100 m from the proposed accelerator.

For all types of projectiles, except deuterons, the following radiological safety recommendations are made for K-500 cyclotron:

1. For the cyclotron vault following are the specifications of minimum shield thicknesses

    (a) **roof** 2.0 m of ordinary concrete or equivalent.

2. For the experimental caves following are the specifications of minimum shield thicknesses

    (a) **roof** 1.0 m of ordinary concrete or equivalent.

3. The 2.2 m square opening in the roof directly above the cyclotron should be shielded on all sides and on the top with 1 m thick ordinary concrete or equivalent. The structure should have a complete enclosure except for a labyrinth entrance on one side.
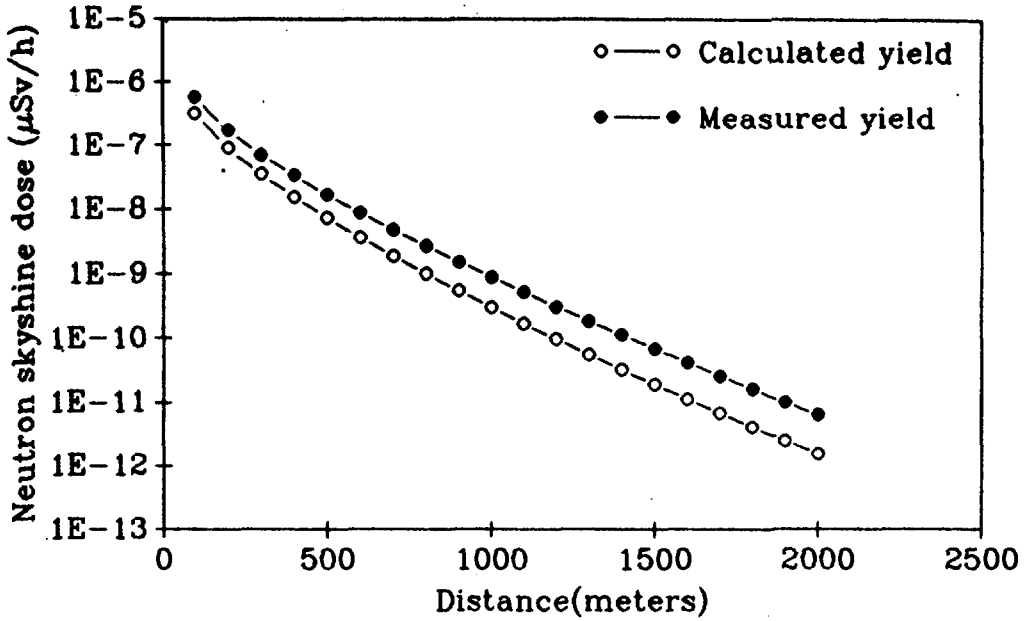
Figure 4.1: Skyshine dose rate at various distances for VECC roof thickness and for 50 MeV α on Ta produced neutron yield.
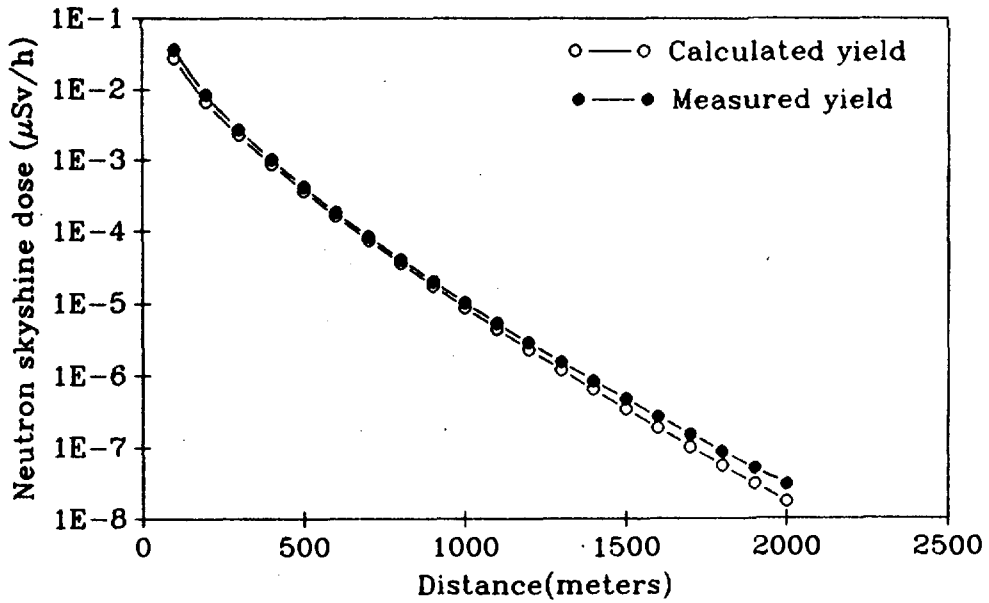

Figure 4.3: Same as figure 4.1 but for no roof condition.

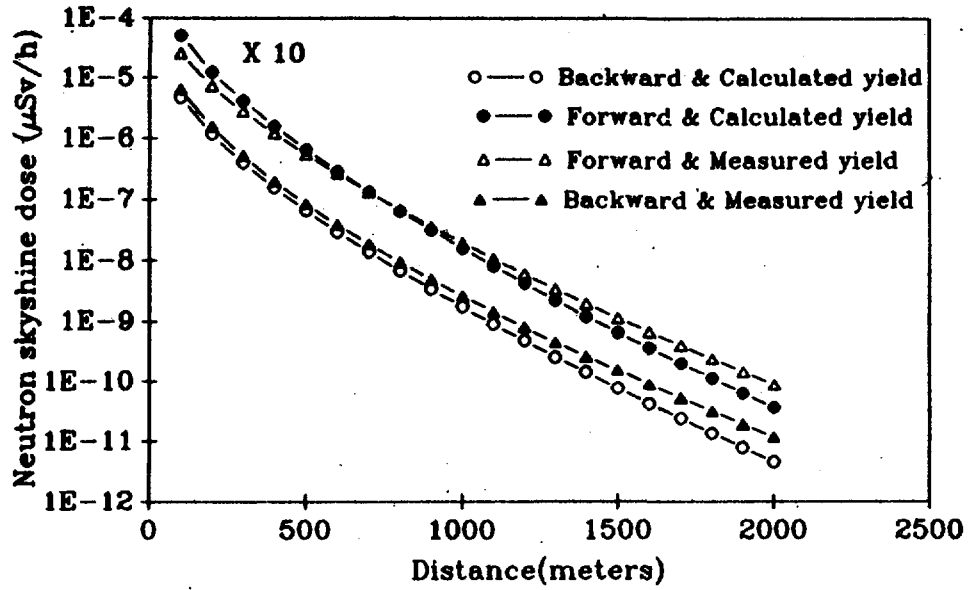**Note: Forward reuslts multiplied by 10**

Figure 4.2: Skyshine dose rate same as Figure 4.1, but for
one planck removal in extreme forward, extreme backward
and also for 50 MeV α on thick Ta for both measured and
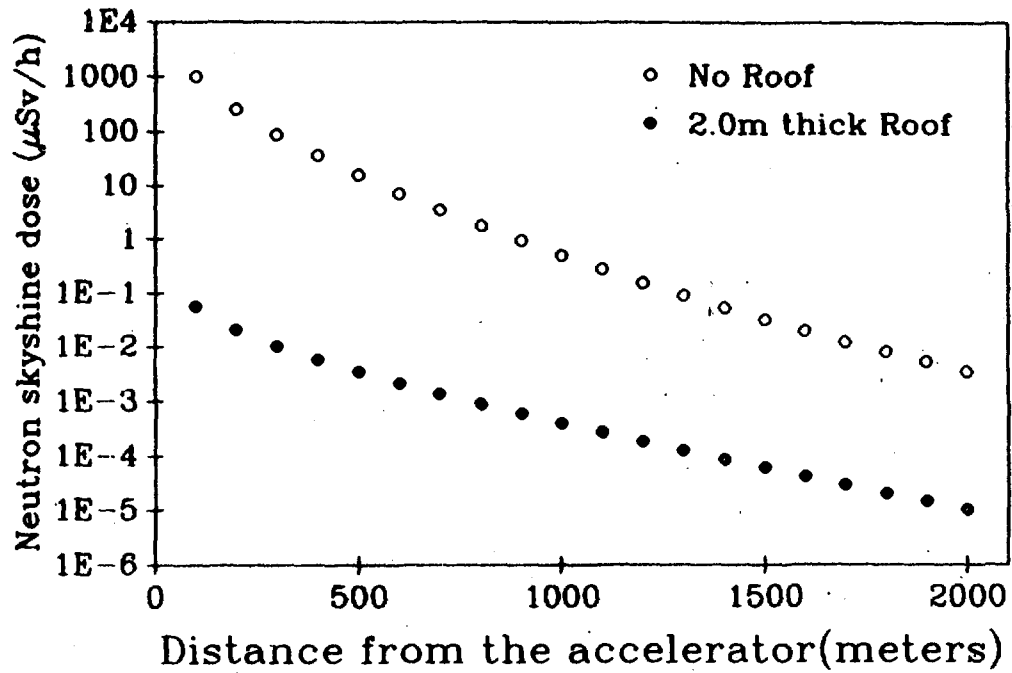calculated neutron yield.

Figure 4.4 Skyshine dose rate at several distances from the accelerator for 500 MeV lithium (50 pnA).

5 Analysis of Neutron Skyshine Dose

In this section a detailed analysis of neutron skyshine with respect to the several possible parameters was carried out. Neutron dose at various distances was calculated (Prabhakar Rao and Sarkar, 1994) using Eq. 2.9 for neutrons produced by 20 μ-ampere beam of 50-MeV and 60-MeV alphas bombarded on thick tantalum targets. Both measured (Sarkar et. al., 1991) and calculated neutron yield distribution were used to estimate the dose. Figures 5.1a and 5.1b show the skyshine dose at distances ranging from 100 m to 2000 m for neutrons transmitted through roof thicknesses 0.4 m to 2.4 m at the step of 0.4 m, for 60-MeV and 50-MeV alphas incident on thick tantalum targets and for measured data using NE-213. The calculation geometry is assumed to be similar to that of VECC, as described in section 4. Similar curves for the calculated neutron yield data using PRECO-D2 are shown in Figures 5.2a and 5.2b. For both the measured and calculated neutron yields the skyshine dose rates are small compared to the natural background radiation dose rates ($0.1\mu Sv/h$) and are smoothly decreasing functions of distance. With increasing roof thickness the dose at a certain distance decreases though the nature of the curve remains the same. However, the dose at any point shows higher value with measured data than with the calculated one. Figure 5.3 shows a comparison of skyshine dose calculated and measured data for 2.4 m roof thickness and for 50-MeV and 60-MeV alphas. This discrepancy may arise due to two reasons:

(i) the interpolation using Eq. 3.12/3.16 may be erroneous;

(ii) the measured and calculated neutron yield distributions may be different.

In figures 5.4a and 5.4b, we show the original as well as for the data calculated using the fitted expressions for 50-MeV and 60-MeV alpha projectiles. The data are shown for 60^0 and 90^0 since these are the angles of interest for our calculations.

Some differences are observed between the fitted and original data but they do not totally account for the observed discrepancy in the final results.

Next, in figure 5.5 we show the calculated and the measured neutron yield distributions for 50-MeV and 60-MeV alpha projectiles respectively for thick tantalum targets. We observe significant differences especially at high neutron emission energies. This difference becomes negligible if we consider the energy integrated total number of neutrons emitted. However the high energy neutrons are likely to contribute more towards the dose. This is evident from Figures 5.6a and 5.6b where the energy distribution of neutron dose is plotted at 100 m, 1000 m, 2000 m for the transmission through a roof of thickness 0.4 m and 2.4 m respectively. The source neutron dose distribution is also plotted along with. It is observed that though the dose distribution of the source decreases with increasing energy, it is not so with transmitted dose distribution. The transmitted dose distribution shows very significant relative contribution from high energy neutrons. This trend is more enhanced at large distances. The relative contribution from high energy neutrons increases with increasing roof thickness. The difference in the neutron flux at high energies between measured and calculated source energy spectra thus accounts for the difference in the total skyshine dose.

It can thus be concluded that the high energy neutrons are important for skyshine dose especially at the large distances. In accelerator produced neutrons high energy neutrons are mainly contributed by the pre-equilibrium part of the nuclear reaction yield. In figures 5.7a and 5.7b we plot the fraction of pre-equilibrium dose i.e., the ratio of the dose from pre-equilibrium neutrons to the total dose at various distances for different roof thicknesses respectively for 50-MeV and 60-MeV alpha projectiles. We have considered here that neutrons with energies 10-MeV and above are originating from the pre-equilibrium part of the reaction mechanism. It is observed that pre-equilibrium neutrons contribute significantly to the total dose especially at large distances. For example, at 2000 m from the source the pre-equilibrium contribution is about 80% or more. This relative contribution increases significantly with increasing roof thickness and projectile energy. For 60-MeV alphas and for 2.4 m roof thickness

almost all the neutron dose is contributed by the pre-equilibrium neutrons. This is because the high energy pre-equilibrium neutrons have more penetrating power both through concrete and air. In calculating the neutron yield distribution it is therefore necessary to estimate the pre-equilibrium part accurately.

The observed difference in the calculated and measured neutron yield at high energies may be due to the following two inadequacies of the pre-equilibrium model used. For alpha projectiles the pre-equilibrium emission spectra depends significantly on the initial exciton configuration (p, h). We have assumed in the present calculations that the initial configuration $p=5$ and $h=1$, which implies that the incident alpha is removed from the entrance channel by interacting with a target nucleon to create a particle-hole pair. Another way the incident alpha can interact with the target nucleus is by its complete dissolution into four nucleons in the nuclear force filed. In this case the initial exciton numbers are $p=4$, $h=0$. The second choice of the initial configuration increases the pre-equilibrium cross-section appreciably (Sarkar et. al., 1991). However, the increase is not sufficient to account for the total discrepancy between the measured and calculated spectra. Generally, an admixture of the calculated spectra from the two configurations is supposed to simulate the actual reaction mechanism involved.

Secondly, we have considered here only single pre-equilibrium emission. It is highly probable that all these excitations more than one pre-equilibrium neutrons will be emitted. Consideration of multiple pre-equilibrium emissions will definitely enhance the high energy part of the calculated neutron spectrum.
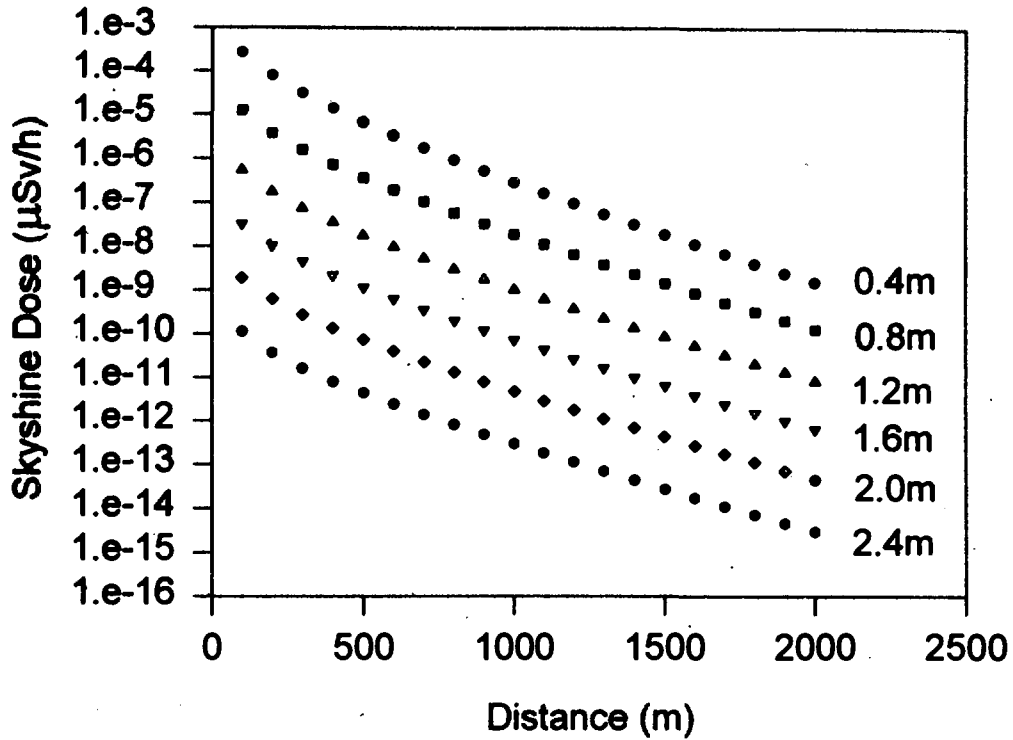
Figure 5.1a: Skyshine dose rates for 20-μA beam of 50 MeV α on Ta and for measured neutron yield.
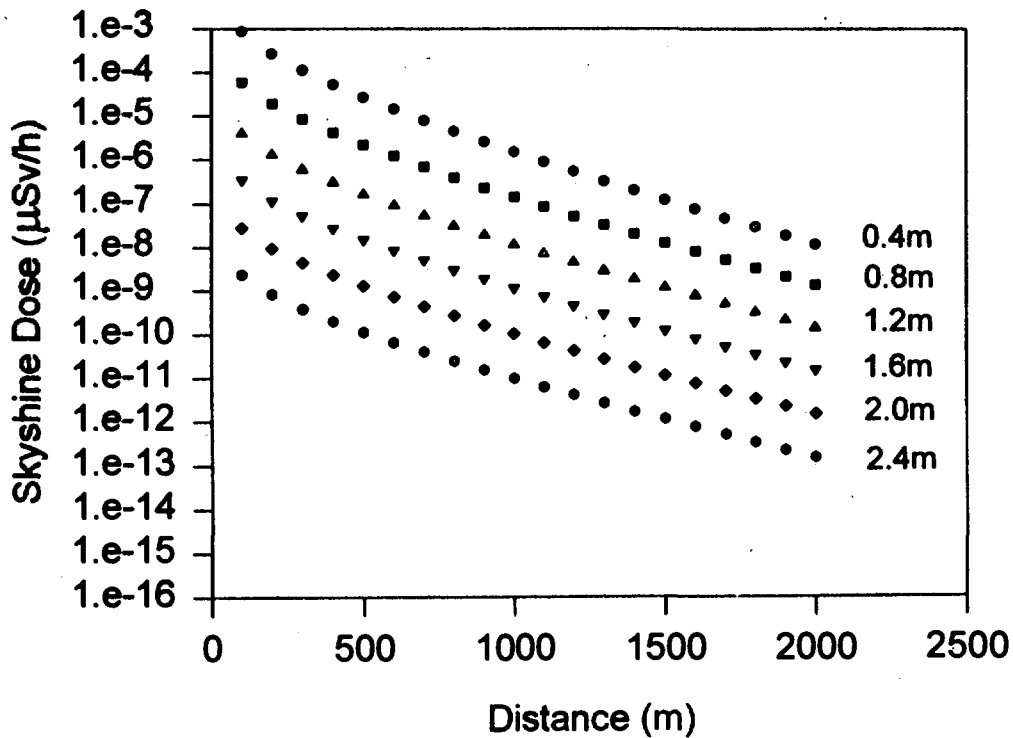

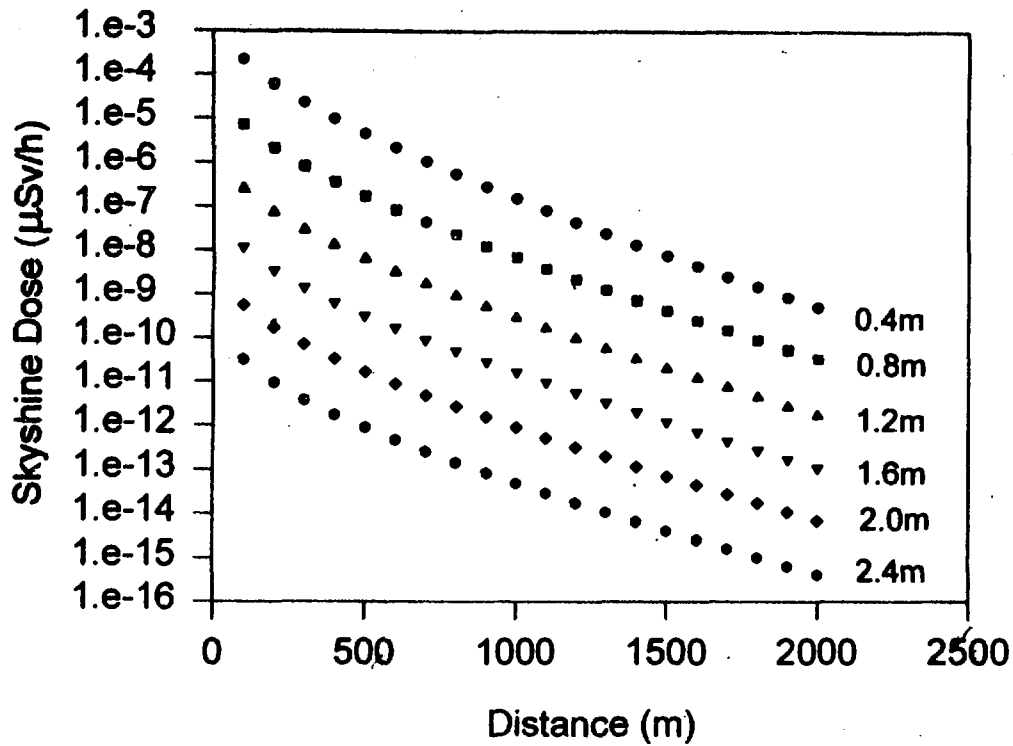Figure 5.1b: Same as Figure 5.1a but for 60 MeV α projectiles.

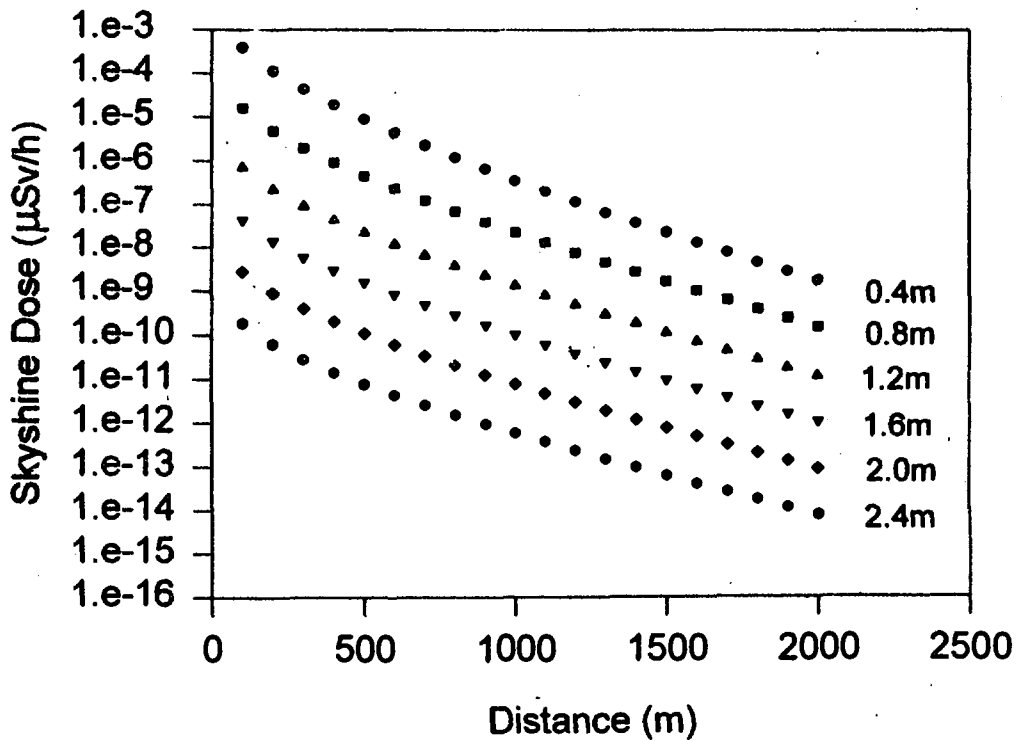Figure 5.2a: Same as Figure 5.1a but for calculated neutron yield.

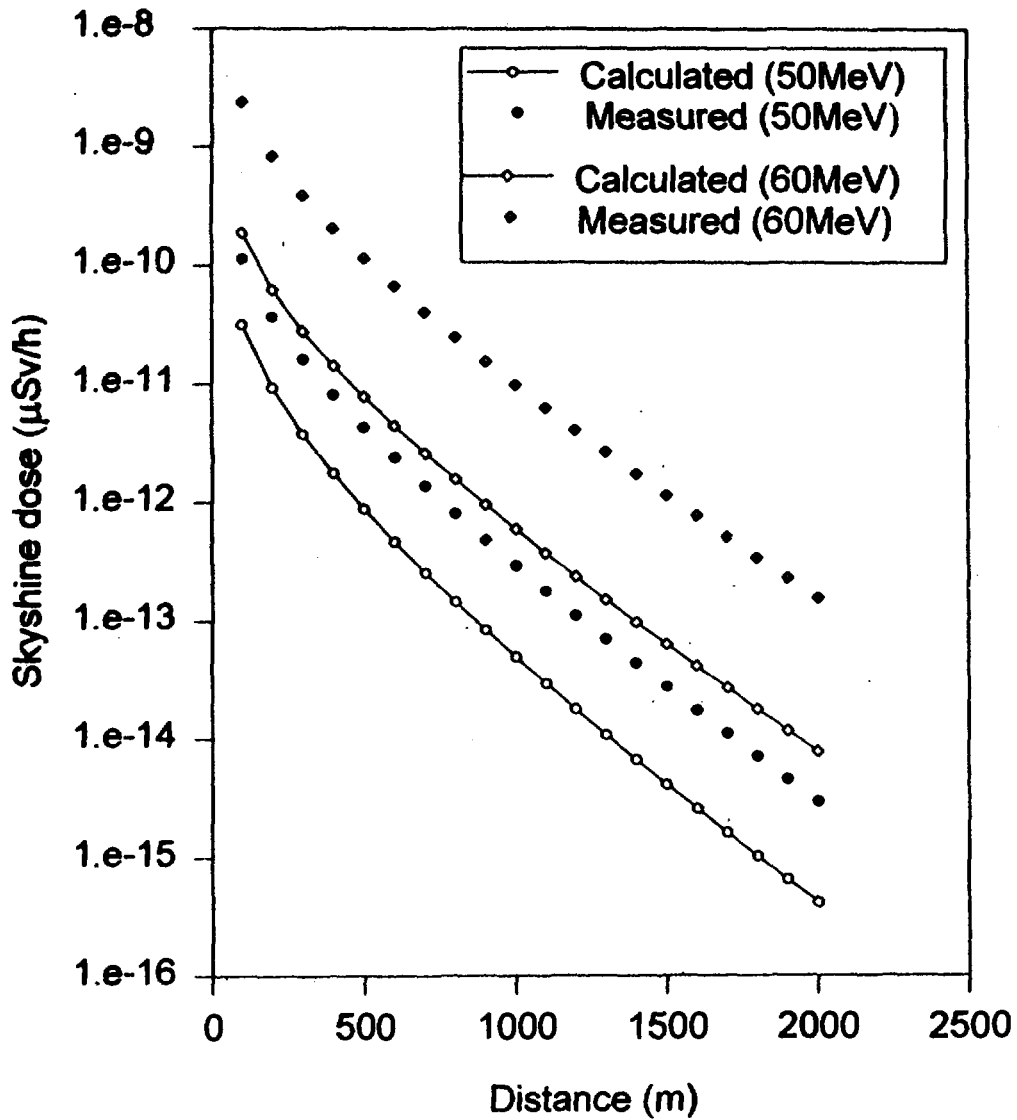Figure 5.2b: Same as Figure 5.1b but for calculated neutron yield.

Figure 5.3: Comparison of skyshine dose at various distances
for 2.4m roof thickness, for measured
and calculated neutron yield distributions and for
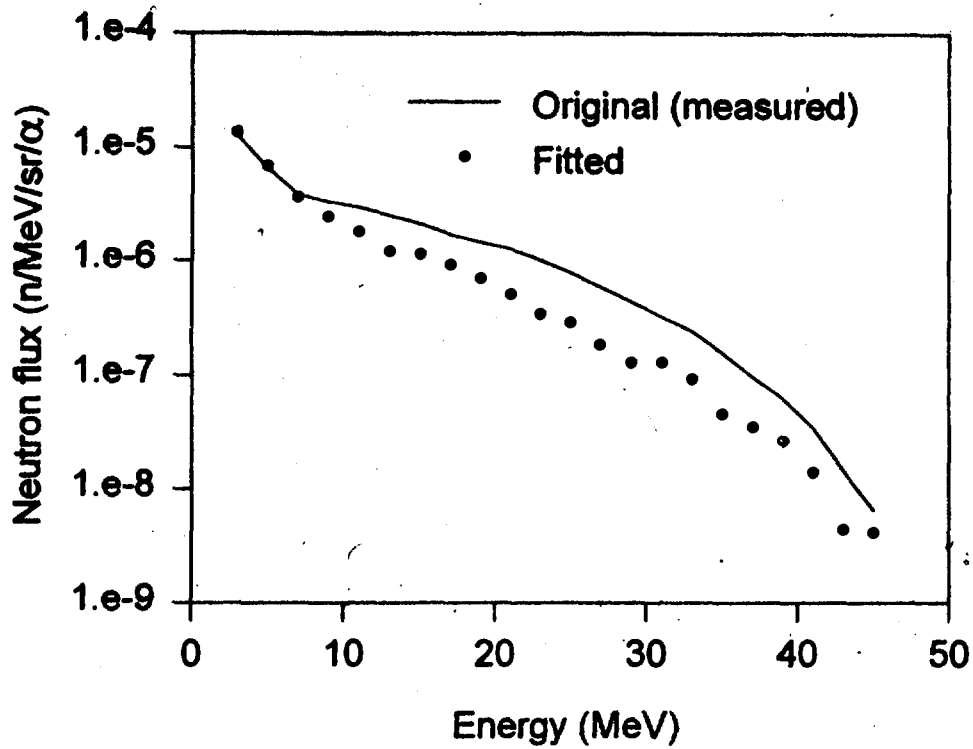50 & 60 MeV α projectiles on thick Ta target.

Figure 5.4a: Comparison of the original (measured) as well as fitted using (Eq. 3.12) neutron yield distributions at 60° for 60 MeV α projectiles on thick Ta target.
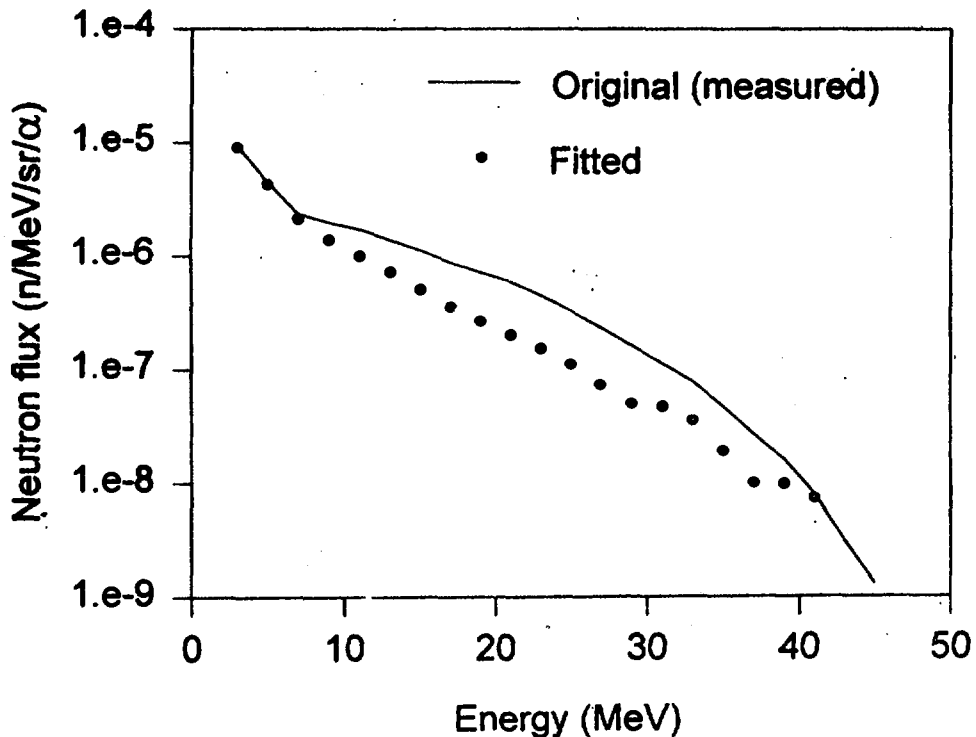

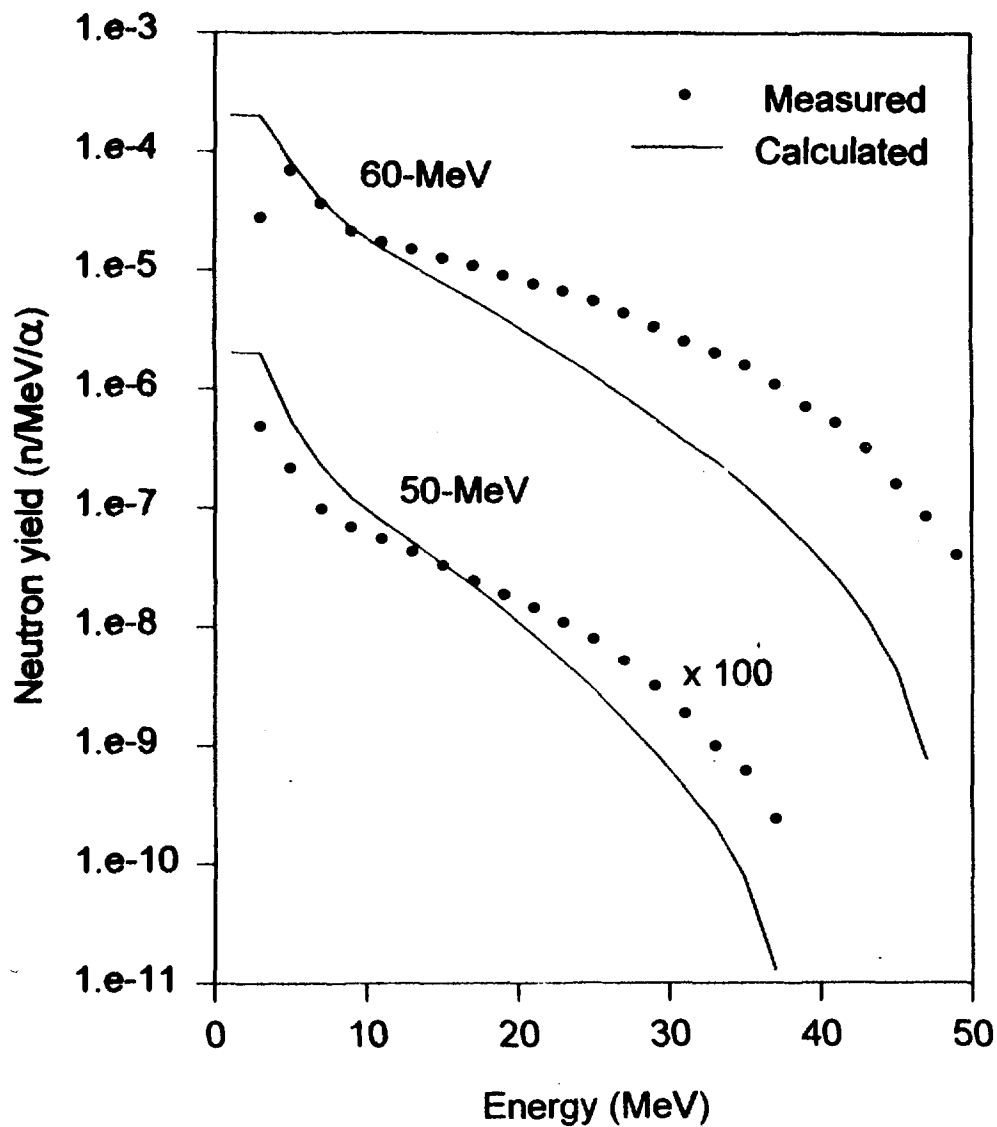Figure 5.4b: Same as Figure 5.4a but for 90°.

Figure 5.5: Comparison of measured and calculated neutron
distributions (angle-integrated) for 50 and 60-MeV
α projectiles on thick Ta target. The data for 50-MeV
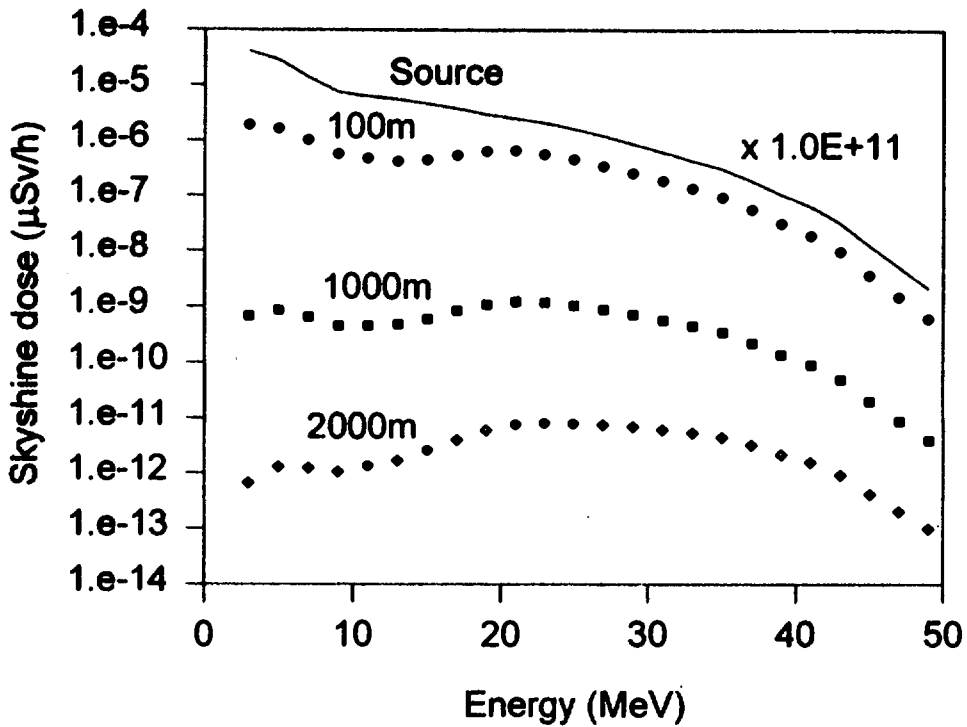α is multiplied by 100.

Figure 5.6a: Comparison of dose distributions at distances
of 100, 1000, 2000 meters with that of the source
neutrons (measured) for 0.4m roof thickness and
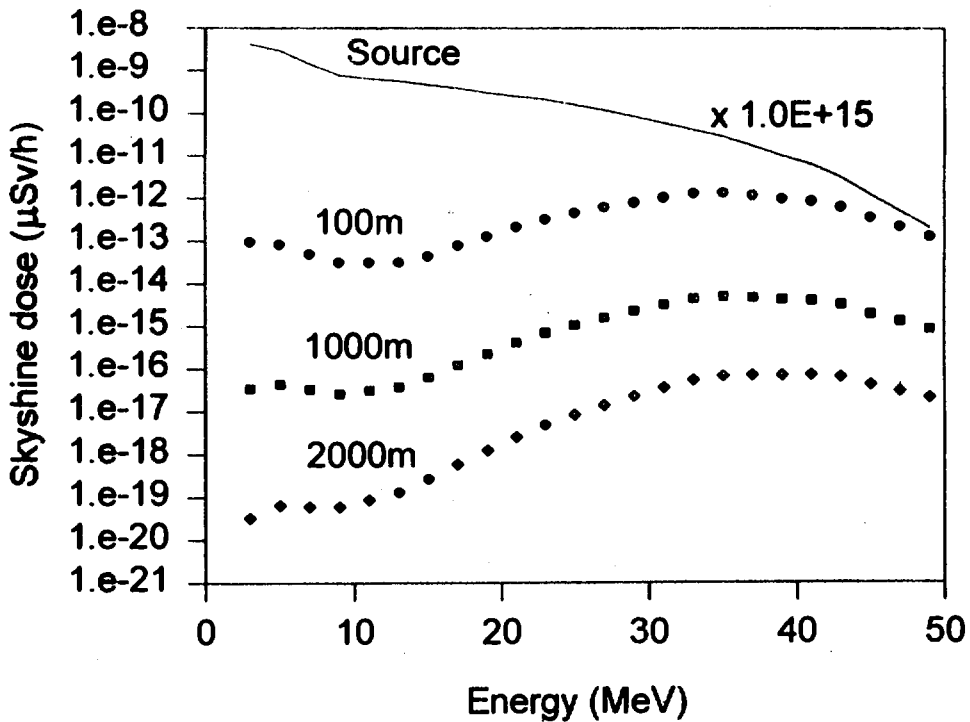60 MeV α projectiles on thick Ta target.

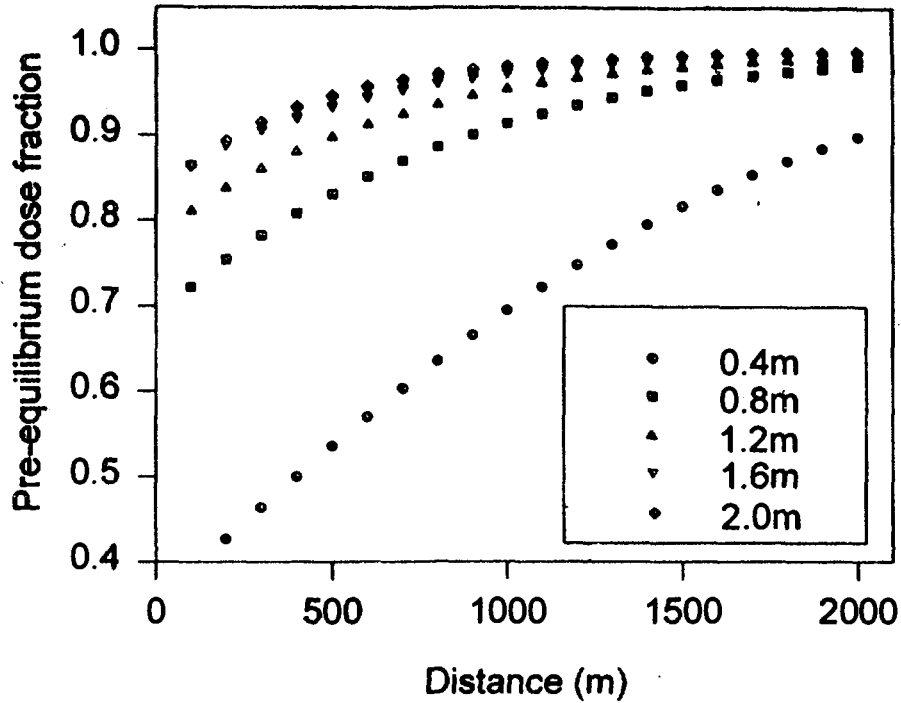Figure 5.6b: Same as figure 5.6a but for 2.4m roof thickness.

Figure 5.7a: Fraction of pre-equilibrium dose (ratio of dose rate due to pre-equilibrium neutrons and total dose for all neutrons) at different distances and different roof thicknesses and for 50 MeV α projectiles on thick Ta target (measured).
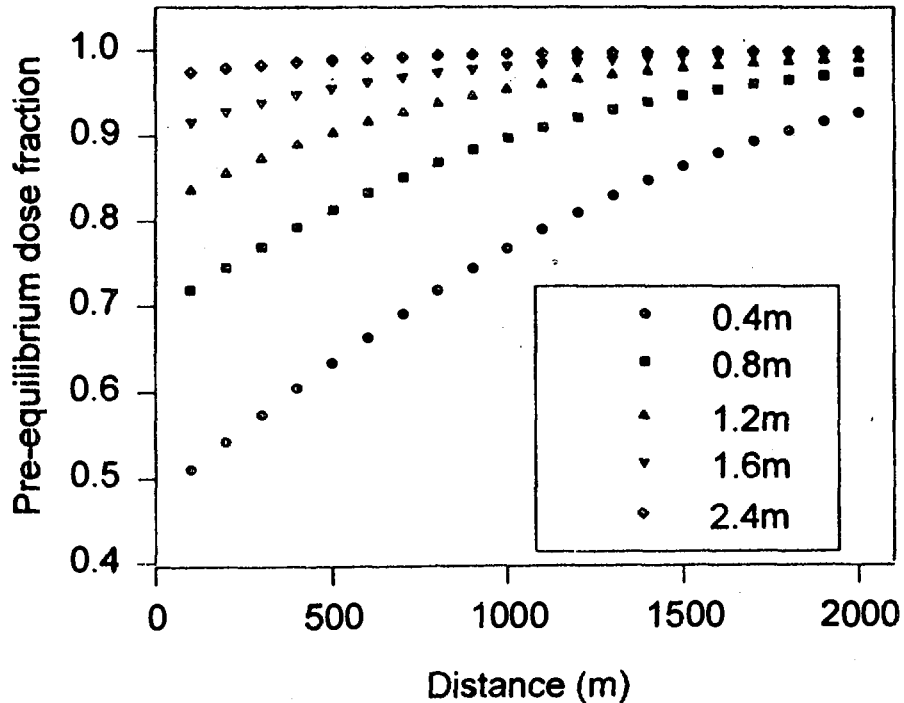

Figure 5.7b: Same as Figure 5.7a, but for 60 MeV α.

6 Conclusion

A simple and inexpensive algorithm for a fast and inexpensive calculation of neutron skyshine dose from particle accelerator facilities is described. Numerical results are obtained at various distances (100–2000m) from the accelerator neutron source for different roof thicknesses and for 50- and 60- MeV α incident on Ta targets. A study of the variation in the neutron skyshine dose with respect to roof thickness and source neutron energy distribution is made. The results indicate that neutron dose at large distances is sensitive to the high energy component of the source neutrons and thereby to the energy of the accelerated ions.

7 References

1. Alsmiller R G Jr., and Barish J. (1978) Neutron-Photon multigroup cross-sections for neutron energies$\leq$ 60 MeV. Report ORNL-TM-6486, Radiation Shielding Information Centre, ORNL, Oak Ridge, TN.

2. Alsmiller R G Jr., and Barish J. (1981) Neutron-Photon multigroup cross-sections for neutron energies$\leq$400 MeV. Report ORNL-TM-7818, Radiation Shielding Information Centre, ORNL, Oak Ridge, TN.

3. Alsmiller R G Jr., Barish J., and Childs R L., (1981) Skyshine at neutron energies $\leq$400 MeV, Particle Accelerators, Vol. 11, PP 131-141, Gordon and Breach, USA.

4. Blann M. (1991) ALICE91-Statistical model code system with fission competition, ORNL Report PSR-146, Oakridge National Laboratory, Oak Ridge, TN.

5. Case K M , Hoffman F De, and Placzek (1953), Introduction to the theory of Neutron Diffusion, Vol. 1, Los Alamos.

6. Gopinath D V., and Santhanam K. (1971) Nucl. Sci. Engng 43, 186.

7. Hack R C, Health Physics (1966), PLA progress report for RHEL R/136, edited by C.Natty and J.M.Dickson, Chapter 9.

8. Hayashi K, Nakamura T (1985), Nucl. Sci. Engg. 91 pp. 332-348.

9. Hayashi K, Nakamura T (1984), Nucl. Sci. Engg. 87 pp. 123-135.

10. Health physics report (1995) A brief report on the radiological saftey considerations of the proposed K=500 Superconducting cyclotron at Calcutta, India (unpublished).

11. IAEA (1988), IAEA Technical Report Series No. 283, Radiological Safety Aspects of Proton Accelerators, IAEA, Vienna.

12. ICRP-21 (1973), Data for protection against ionising radiation from external sources : supplement to ICRP publication 15, ICRP publication 21 OXFORD: Pergamon press.

13. ICRP-60 (1990), ICRP 60 recommendations, OXFORD: Pergamon press UK.

14. Kalbach C, Mann F M (1981) Phy. Rev. C. 23 pp. 112.

15. Kalbach C (1985) PRECO-D2: A programme for calculating pre-equilibrium and direct reaction double-differential cross-sections, Los Alamos, National Laboratory Report, LA-10248-MS.

16. Kalbach C. (1988) Phys. Rev. C 37, 2350.

17. Kalbach C. (1993) Nucl. Sci. Engg. 115, 43.

18. Kinney W E (1962), Oak Ridge National Laboratory Report, ORNL-3287, USA.

19. Ladu M, Pelliccioni M, Picchi, and Verri G (1968), A contribution to the skyshine study, Nucl. Instrum. Methods, 62, pp. 51.

20. Lindenbaum S J (1957), Proceedings of the conference on shielding of High energy accelerators TID-7545, NEW YORK, pp. 28 and 101.

21. Lindenbaum S J (1961), Ann. Rev. Nucl. Sci. 11, pp. 213.

22. Nakane Yoshihiro et. al., (1997) Intercomparison of Neutron Benchmark Analyses for Iron and Concrete shields in low, intermediate and high energy proton accelerator facitlities, SATIF-3, tokyo, Japan.

23. Nakamura T, Kosako T (1981a), Nucl. Sci. Engg. 77, pp. 168-181.

24. Nakamura T, Kosako T, Hayashi K, Ban S, Katoh k, (1981b) Nucl. Sci. Engg., pp. 182-191.

25. Nakamura T., Fuji M., Shin, K. (1983) Nucl. Sci. Engng 83, 444.

26. Nakamura T, Uwamino Y, Hayashi K, Torii A, Ueda M, Takahashi A, (1985) Nucl. Sci. Engg., 90, pp. 281-297.

27. NCRP (1977), National Council on Radiation Protection and Measurements, Radiation Protection Guidelines for 0.1-100 MeV particle accelerator facilities. NCRP Report No. 51 (Washington : National Council on Radiation Protection and Measurements.)

28. Patterson H W, Thomas R H (1973) Accelerator Health Physics New York and London, Academic Press.

29. Prabhakar Rao G, and Sarkar P.K, (1993a) A study of the variation of air-scattered neutron dose with respect to roof thickness, roof distance and source spectrum, Proceedings of NSRP-10, IGCAR, Kalpakkam, India.

30. Prabhakar Rao G, and Sarkar P.K, (1993b) Calculation of neutron skyshine dose from the variable energy cyclotron, Proceedings of the PATPAA-93, IUC-DAEF, Calcutta, India.

31. Prabhakar Rao G. and Sarkar P.K, 1994, Estimation and analysis of neutron skyshine dose from particle accelerators, Annals of Nuclear Energy Vol. 21, pp.11-18.

32. Prabhakar Rao G. and Sarkar P.K, (1995a), A study of the variation of neutron skyshine dose with respect to roof thickness, source neutron spectrum distribution, Journal of Testing and Evaluation JTEVA, Vol.23, No.5, 388 ASTM, USA.

33. Prabhakar Rao G, and Sarkar P.K ,(1995b) Sensitivity studies of air-scattered neutron dose from particle accelerators, Proceedings of the international symposium, SAMO-95, Beligrate, Italy.

34. Prabhakar Rao G, and Sarkar P.K, (1996) Transport of accelerator produced neutrons through ordinary concrete, Proceedings of the National conference on

Radiation shielding and protection, IGCAR, Kalpakkam, India (Allied publishers limited, New Delhi, India).

35. Prabhakar Rao G, and Sarkar P.K, (1997a) A modified code system for the transport of accelerator produced neutrons, Annals of Nuclear Energy Vol. 24, pp. 575-586.

36. Prabhakar Rao G, and Sarkar P.K, (1997b) Sensitivity studies of air scattered neutron dose from particle accelerators, J. Statist. Comput. Simul. Vol. 57, pp. 261-270.

37. Ramakrishna Rao A, 1986 MSc. Thesis, Bombay University, Bombay, INDIA.

38. Rindi A, Thomas R H (1975) Particle Accelerator. Vol. 7, pp. 23.

39. Roussin R W., Alsmiller R G Jr., and Barish J. (1972) Calculations of the Transport of Neutrons and secondary gamma rays through concrete for incident neutrons in the energy range 15 to 75 MeV. Report ORNL-TM-3659 (revised), Radiation Shielding Information Centre, Oak Ridge, TN.

40. Sarkar P K, Bandyopadhyay T, Muthukrishnan G, Ghose Sudip (1991) Phy. Rev. C.43, pp. 1855.

41. Sims C S., and Killough G G. (1983) Radiat. Prot. Dosim. 5, 45.

42. Stevenson G R, Thomas R H (1984), Health Physics. Vol.46, pp. 115.

43. Trubey D K, Comolander H E (1971) A Review of calculations of Radiation Transport in Air ORNL-RSIC-33, Radiation Shielding Information Centre,Oak Ridge National Laboratory.

44. Williamson C F, Bonjot J P, Picard J (1966) Centre Etudes Nucleaires de Saclay Report CEA-R 3042.

45. Weisskopf V. F. and Ewing D. W (1940) Phys. Rev. 57, 472.